STUDY OF HETEROJUNCTION $Pb_{1-x}Sn_xTe$ DIODES

Jose Manuel Fernandez

NAVAL POSTGRADUATE SCHOOL
Monterey, California

THESIS

STUDY OF HETEROJUNCTION $Pb_{1-x}Sn_xTe$ DIODES

by

Jose Manuel Fernandez

Thesis Advisor: T. F. Tao

December 1972

Study of Heterojunction $Pb_{1-x}Sn_xTe$ Diodes

by

Jose Manuel Fernandez
Lieutenant, Chilean Navy

Submitted in partial fulfillment of the
requirements for the degree of

MASTER OF SCIENCE IN ELECTRICAL ENGINEERING

from the

NAVAL POSTGRADUATE SCHOOL
December 1972

ABSTRACT

A new procedure of using metal rich $(Pb_{1-x}Sn_x)_{1+\delta}Te$ alloy source in a graphite boat deposition method has been developed in preparing n-type $Pb_{0.8}Sn_{0.2}Te$ thin films of carrier concentration in the low 10^{17} cm^{-3} range without annealing. Using this procedure, single heterojunction $Pb_{1-x}Sn_xTe$ diodes have been made by sequential depositions of p-type $Pb_{0.86}Sn_{0.14}Te$ and n-type $Pb_{0.80}Sn_{0.20}Te$ thin films on cleaved (100) KCL substrates. Diodes were made by using gold deposition and silver epoxy contacts. Rectifying diodes of R_oA values as high as 600 ohm-cm^2 have been obtained.

A theoretical analysis was carried out in calculating the laser performance of a double heterojunction $Pb_{1-x}Sn_xTe$ diodes. Its results will be used as guidelines for continuing experimental research and development.

It was calculated that at liquid nitrogen temperature, lasing threshold is between 200 to 300 amp/cm^2 and power output in the milliwatt range can be achieved with moderate biasing.

ACKNOWLEDGEMENTS

I would like to acknowledge and deeply thank Professor T. F. Tao for the personal encouragement and many suggestions received during the course of his supervision of this thesis, as well as his support that made possible the realization of many experiments and analysis.

Special thanks to Dr. H. McMillan and S. Chang of Standford University for the use and help in some of the heterojunction experiments made in their laboratory.

I would like to thank R. Zahm and M. Jaehnig for their cooperation and assistance in the development of the experiments in our laboratory.

Also, thanks to the Machine Shop Facility of the Naval Postgraduate School for their contribution in the construction of the multi-source system. I extende my acknowledge to W. Neial for his helpful assistance in the use of general equipments.

The partial support of the Office of Naval Research and the Air Force Materials Laboratory is also acknowledged.

TABLE OF CONTENTS

LIST OF TABLES

LIST OF FIGURES

I. INTRODUCTION

A. INTRODUCTION

$Pb_{1-x}Sn_xTe$ alloy semiconductor has been actively developed in recent years because of the unique property that its energy gap can be made small, even approaching zero, by changing the alloy composition and temperature. Consequently, it has become an important semiconductor for applications in long wavelength infrared (LWIR) spectrum, notably in the 8 to 14 microns atmospheric window for imaging, surveillance, remote sensing, thermography applications and also for use in the 10.6 microns CO_2 laser systems. Practical LWIR devices using $Pb_{1-x}Sn_xTe$ have been quite well developed. They are all based on a p-n homojunctions and have adequate device performances for some practical applications when used as photovoltaic detectors and as semiconductor lasers. Recently, heterostructure devices of 3-5 alloy semiconductors have shown much improved lasing and solar cell (photovoltaic) performances compared with their homojunction counterparts. It is the purpose of this thesis to initiate a research effort to investigate if similar improvements can be achieved in Pb-Sn-Te heterojunctions devices also.

B. TOPICS OF THIS THESIS

To initiate this research program in developing hetero-4-6 alloy semiconductor devices for LWIR applications, two projects were identified for this thesis.

1. Theory

A theoretical study was carried out to investigate the possible improvements of the laser performance in a double heterojunction $Pb_{1-x}Sn_xTe$ laser diode. The alloy compositions selected were X=0.14 and 0.20. At 77°K, their energy gaps are 0.135 and 0.105 ev. corresponding to photon energies of 9.18 microns and 11.8 microns infrared radiations respectively. The purpose is to determine the effects of the alloy composition, thickness and carrier concentration of the different layers in a double heterojunction laser on lasing threshold current, external differential quantum efficiency and power output. This result can serve as a guide for the experimental research program in developing more efficient heterojunction $Pb_{1-x}Sn_xTe$ lasers.

2. Experiment

An experimental program was started to develop a thin film deposition process to fabricate $Pb_{1-x}Sn_xTe$ heterojunction devices and to evaluate their metallurgical, electrical, photovoltaic and optoelectronic properties. For this thesis, attentions were limited to the preliminary development of thin film deposition process for producing reproducible n type and p type layers and also to establishing the feasibility of fabricating rectifying $Pb_{1-x}Sn_xTe$ hetrojunction devices.

II. BACKGROUND

A. $Pb_{1-x}Sn_xTe$ NARROW GAP SEMICONDUCTOR

$Pb_{1-x}Sn_xTe$ is a binary alloy with rocksalt structure, with the special property that the energy gap is a strong function of the composition, temperature and pressure. By controlling these parameters, it is possible to tailor the energy gap to small valves. Consequently, it is an important semiconductor in the infrared region. The ease in producing good single crystals with quality and homogeneity has made it possible to fabricate infrared detectors as well as junction lasers.

The change of energy gap with the composition and temperature for the $Pb_{1-x}Sn_xTe$ alloy series, was explained by Dimmock [1], in the so called band inversion model. Strong experimental evidence revealed that this model can be applied to the following types of alloy:

a. $Pb_{1-x}Sn_xTe$

b. $Pb_{1-y}Sn_ySe$ [2, 3]

c. $Pb_{1-z}Sn_zS$ [4]

d. $(PbSe)_{1-x}(SnTe)_x$ [5]

Experimentally, this model was inferred from laser emmission at low temperatures [1, 6], optical absorption edges [7, 8, 9], photovoltaic thresholds [10], photoconductive thresholds [11], results from tunneling experiments [12] and from the electrical data near the band crossing composition for the crystals with low carrier concentrations [13].

$Pb_{1-x}Sn_xTe$ have been more intensily developed in the last few years, with centered attention focused on the bulk crystals. The growth techniques used, had been the liquid epitaxy [17], Czochralski [16], open-tube vapor growth [15], closed-tube growth [14], and Bridgman [14]. Single crystals grown by Bridgman techniques and the vapor phase are high quality single crystals which exhibit (100) cubic structures. The asgrown crystals all have high carrier concentrations, which must be annealed in order to obtain device quality materials for the devices.

The crystal structure for $Pb_{1-x}Sn_xTe$ alloys, is the Bl rocksalt, throughout the whole composition range.

B. HETEROJUNCTION DEVICES

1. Introduction

A heterojunction is a junction formed between two different semiconductors. They can have different energy gaps or they can be the same type of semiconductor but different dopings, such as in $n-n^+$; $p-p^+$ heterojunctions.

The early work was done on Ge-Si and Ge-Ga AS heterojunctions. A large number of other heterojunctions have also been studied such as InP-GaAs, GaP-GaAS, In As-GaAs, InSb-GaAS-GaSb, InSb-GaSb, etc. These heterojunctions were mostly the combination of group 4 and 3-5 compounds, Considerable research have been done but no device with good enough performance for practical applications can be developed until heterojunctions using alloy semiconductors were developed. Two outstanding examples

are the GaAS-$GaAs_{1-x}P_x$ and GaAs-$Ga_{1-x}Al_xAs$ heterojunctions. The $Ga_{1-x}Al_xAs$ heterojunctions are worthy of special emphasis because it significantly changes the semiconductor laser field from a research laboratory interest to a promising practical device for system applications.

Heterojunctions of 2-6 compounds and alloys have also been extensively studied. Probably because the difficulty of preparing both good n type and p type materials in these relatively large energy semiconductors. There has not been any heterojunctions of 2-6 semiconductors having exciting device performance yet.

As for the 4-6 compounds and alloys, whose energy gaps are mostly less than 0.4 ev. which make them very important semiconductors for infrared applications, there is not heterojunction research reported. Although a theoretical analysis of a $PbS_{1-x}Se_x$ double heterojunction laser has recently been completed.

The motivation of this thesis study is to initiate a research in the development of $Pb_{1-x}Sn_xTe$ and $Pb_{1-y}Sn_ySe$ heterojunction devices. If successful, it will undoubtedly make a significant impact on the long wavelength infrared technology same as what $Ga_{1-x}Al_xAs$ heterojunctions have done on the near infrared and visible opto-electronics technology.

In addition to the use of heterojunctions as efficient "close-confinement" injection lasers, other applications are being developed.

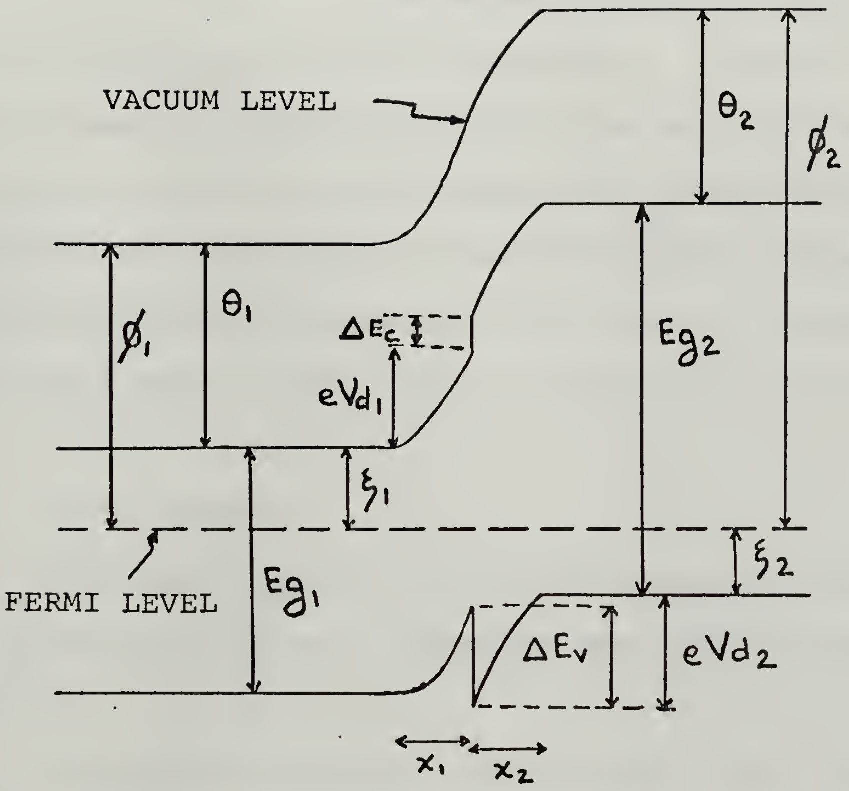

Figure 2.1 HETEROJUNCTION MODEL (IDEAL)

(1) Solar cells
(2) High speed photodetectors
(3) Luminescent diodes
(4) Negative affinity photoemitters
etc.

2. Theory I--Electrical Properties

In the following, three major aspects of the theory of heterojunction devices will be reviewed. They are (a) band diagram, (b) depletion layers and capacitance effect and (c) conduction properties--I-V characteristics. The discussion is limited to n-p heterojunctions which have abrupt profiles, because we believe that the $Pb_{1-x}Sn_xTe$ heterojunctions made in this thesis study belong to such a class.

a. Band Diagram

The band diagram of an ideal abrupt n-p heterojunction is shown in Figure 2-1. which was first proposed by Anderson [18].

The major difference between this band diagram and that of a homojunction are the discontinuities in both the conduction band and valence band. They exist because, at thermal equilibrium, the Fermin level must be constant everywhere inside the device and the vacuum level must be continuous and parallel to the band edge everywhere. Such interface conditions lead to the condition:

Conduction band continuity

$\Delta E_C=(\theta_2-\theta_1)$=difference in the electron affinity of the two semiconductors

$\Delta E_V=(E_{o2}-E_{o1})+(\theta_2-\theta_1)$

Similar to the homojunction case, a space charge distribution is resulted and a contact (or diffusion) potential V_d exist at the junction.

b. Depletion Layers and Capacitance Effect of Ideal Diode Without Interface States

To study the depletion layers, Poisson equations on both sides of the interface are solved. Because the dielectric constants ϵ_1, ϵ_2 are different, the electric field $\mathcal{E}$ is discontinuous at the interface, the electric displacement $\mathcal{D}$ is continuous however. The boundary condition at the interface is, therefore,

$$\epsilon_1 \mathcal{E}_1 = \epsilon_2 \mathcal{E}_2$$

Similar to the analysis of homojunctions, we assume:

(1) no mobile carriers in the depletion layers
(2) Complete ionization of impurities

$$N_D^+ \cong N_D$$

$$N_A^- \cong N_A$$

Let us first consider semiconductor #1.

$$\frac{d\mathcal{E}_1}{dx} = \frac{qN_{D1}}{\epsilon_1}$$

Integrating this equation twice, we get

$$V_{d1}(x) - V_{d1}(-x) = -\frac{qN_{D1}}{\epsilon_1}\left[\frac{x^2}{2} + x_1 x + \frac{x_1^2}{2}\right]$$

Let X=0, we obtain the barrier height in semiconductor #1 as

$$V_{d1} = \frac{qN_{D1}x_1^2}{2\epsilon_1}$$

The depletion layer width at zero bias can be expressed as

$$x_1 = \sqrt{\frac{2\epsilon_1 V_{d1}}{q N_{D1}}}$$

In the case when a bias voltage V is applied, let us assume $V=V_1+V_2$, where V_1, V_2 are the fraction of the bias voltage or side 1 and side 2, then

$$x_1 = \sqrt{\frac{2\epsilon_1 (V_{d1} - V_1)}{q N_{D1}}}$$

Similarly, study of semiconductor #2 side gives:

X_2=depletion layer width in semiconductor 2

$$= \sqrt{\frac{2\epsilon_2 (V_{d2} - V_2)}{q N_{A2}}}$$

It should be noted that V_1 and V_2 are still unknown. They can be determined by the boundary condition at interface

$$\epsilon_1 \mathcal{E}_1 = \epsilon_2 \mathcal{E}_2$$

or the space charge neutrality condition $q\text{-}N_{D1}X_1=qN_{A2}X_2$.

The result is: $$\frac{V_{d1}-V_1}{V_{d2}-V_2} = \frac{\epsilon_2 N_{A2}}{\epsilon_1 N_{D1}}$$

Since $V_d-V=(V_{d1}-V_1)+(V_{d2}-V_2)$, the depletion layer widths can now be expressed in terms of known parameters.

$$x_1 = \sqrt{\frac{2\epsilon_1\epsilon_2 N_{A2} (V_d - V)}{q N_{D1}(\epsilon_1 N_{D1} + \epsilon_2 N_{A2})}}$$

$$x_2 = \sqrt{\frac{2\epsilon_1\epsilon_2 N_{D1} (V_d - V)}{q N_{A2}(\epsilon_1 N_{D1} + \epsilon_2 N_{A2})}}$$

The total depletion width W is:

$$W = x_1 + x_2 = \sqrt{\frac{2\epsilon_1\epsilon_2 (V_d - V)(N_{A2} + N_{D1})^2}{q(\epsilon_1 N_{D1} + \epsilon_2 N_{A2}) N_{D1} N_{A2}}}$$

The junction capacitance can be calculated as:

$$C = \frac{dQ}{dV} = \frac{d(qN_{D1}x_1)}{dV} = \sqrt{\frac{q\epsilon_1\epsilon_2 N_{D1} N_{A2}}{2(\epsilon_1 N_{D1} + \epsilon_2 N_{A2})(V_d - V)}}$$

It should be emphasized that the previous analysis are often modified considerably in practical cases due to the presence of interface states which are caused by the unavoidable lattice mismatch between two dissimilar semiconductors.

c. Conduction Properties--I-V Characteristics

Generally speaking, because of the band discontinuities, the barriers to the two types of carriers have different magnitudes. Current in a heterojunction usually consist mainly of one type of carriers. However, theoretical study of I-V characteristics of a heterojunction is complicated by the presence of interface states. There are three families of theory.

(1) Thermionic emission theory:

If the barrier height $\gg \frac{kT}{q}$, the current density is

$$J = A \exp\left(-\frac{qV_{d2}}{kT}\right)\left[\exp\left(\frac{qV_2}{kT}\right) - \exp\left(-\frac{qV_1}{kT}\right)\right]$$

Using the voltage relation derived in (A), we can express

$$J = J_o\left(1 - \frac{V}{V_d}\right)\left[\exp\left(\frac{qV}{kT}\right) - 1\right]$$

This is very similar to the I-V characteristic of a Schottby barrier diode (metal-semiconductor) but J_o has different temperature dependence and the reverse current increases with V and never saturates. It should be pointed

out that past studies have shown that this thermiomic theory does not account for experimental results very well.

(2) Tunneling theory

(3) Generation recombination (at interface states) theory

Details can be found in Sze's text and will not be reviewed here [19].

3. Theory II--Photoelectric Properties

Although heterojunction devices used as diodes and transistors have been investigated, their importances and contributions lie in optical region. In both semiconductor light emitting diodes and lasers applications, heterojunctions have significantly improved their efficiencies and power outputs. There is no specific result published yet on the improvement of performance when a heterojunction is used as photovoltaic detector. It is believed, however, that improvements in both quantum efficiency and response time can be expected.

Heterojunction concept was originally proposed in the early 60's [20, 21, 22]. However, practical realization of the potential improvement in device performance was not realized until late 60's when closed confinement heterojunction GaAlAs laser diodes fabricated by liquid phase epitaxy method were reported [23]. The lattice constants of GaAs and AlAs are 5.6534 Å and 5.639 Å respectively. This close match apparantly played an influential role in making the GaAlAs alloy the most successful heterojunction devices as LED, semiconductor lasers and solar cells to date.

The basic heterojunction structures are shown in Figure 2-2 which showed three major properties (1) structure (2) energy gap and (3) index of refraction for a homojunction, a single heterojunction and a double heterojunction diodes.

It is believed that there are three mechanisms responsible for the improvements in opto-electronic device performance.

(1) Better optical confinement in junction region and improved optical waveguiding due to the difference in index of refraction between the different semiconductor layers.

(2) Reduced optical absorption loss in the larger energy gap region.

(3) Possibly, enhancement electron confinement when carriers are reflected back into the active region due to the existence of potential barriers.

Several theories have been developed to analyze these mechanisms. In the next chapter, a simplified theory will be used to study the possible improvement in lasing properties of a double heterojunction $Pb_{1-x}Sn_{x}Te$ laser.

Qualitatively, the exciting achievements of the heterojunctions can be vividly highlighted by the following chronological account of the lasing threshold current density J_{th} of GaAs lasers.

(1) When GaAs was first invented, J_{th} was around 100,000 amp/cm^2 in diffused diodes.

(2) The success of liquid phase epitaxy method in fabrication GaAs laser diodes reduced J_{th} to 40,000 to 60,000 amp/cm^2 and improved power efficiencies up to 1%, differential quantum efficiencies up to 10-20%. The operation was mostly pulsed and at crytogenic temperature.

(3) With the success of heterojunction structure, J_{th} as low as 1000 amp/cm^2, differential quantum efficiencies up to 50% have been achieved. Consequently, high duty cycle (even CW) operations at room temperature are now possible.

It is obvious that research efforts should be made to extend such exciting improvements out to infrared wavelength region where important applications such as imaging, surveillance, remote sensing, thermography, 10.6 microns CO_2 laser system developments, all can use improved semiconductor lasers and detectors.

III. THEORETICAL STUDY DOUBLE HETEROJUNCTION $Pb_{1-x}Sn_xTe$ LASERS

A. THEORY OF SEMICONDUCTOR LASERS

1. Introduction

The theory of semiconductor lasers is very complicated because of the following reasons. From the electronic transition or energy conversion point of view, a correct theory must take into account the density of states and the distribution of injected electrons and holes in these states. This presents difficulty in calculating the optical gain. From the radiation propagation point of view, the complication arises because the electromagnetic wave analysis in a semiconducting medium with a varying dielectric constant simply has not been done. This presents difficulty in calculating the optical loss.

However, approximations have been proposed and simplified theories have been carried out to analyze semiconductor lasers. Fortunately, one of the simplified theories has received some experimental verifications in spite of the drastic assumptions made in its theoretical development [24].

2. Optical Gain in Semiconductor Lasers

Although the electronic population in a semiconductor is distributed over a continuoum in either the conduction or valence band, the simplified semiconductor laser theory still uses the Einstein treatment of induced and spontaneous

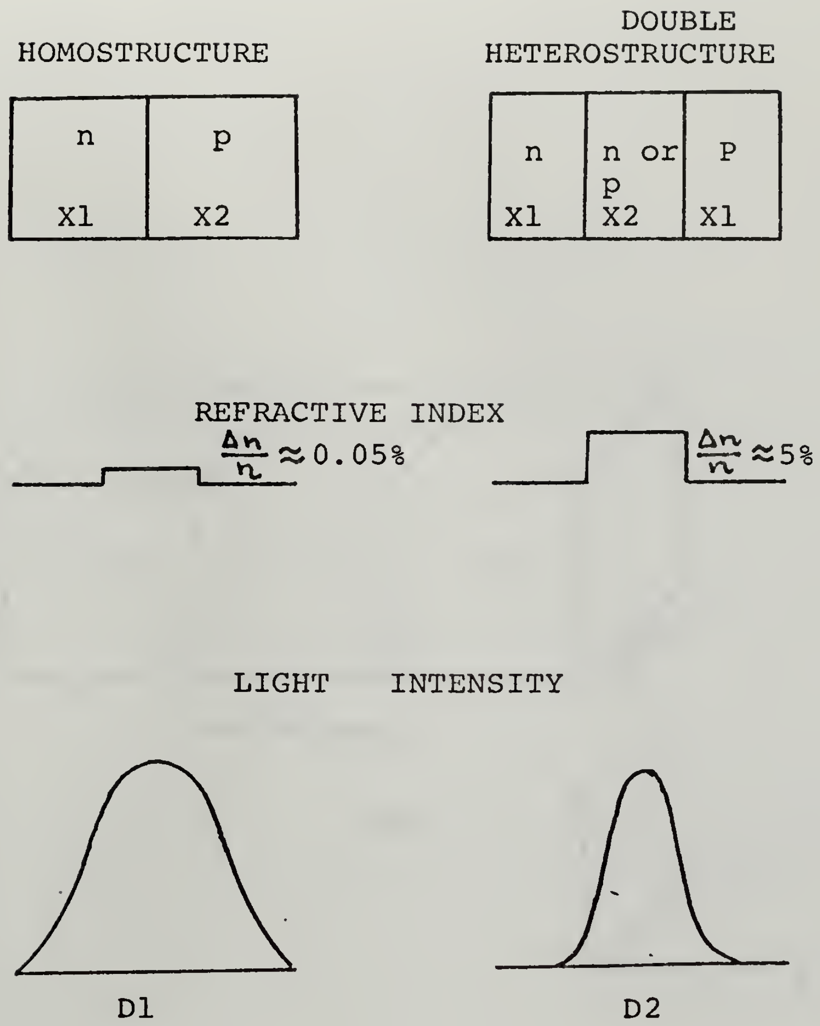

X1=Composition of tin in the first material
X2=Composition of tin in the second material

Figure 3.1 Light Intensity Characteristic for Homo and Heterojunction

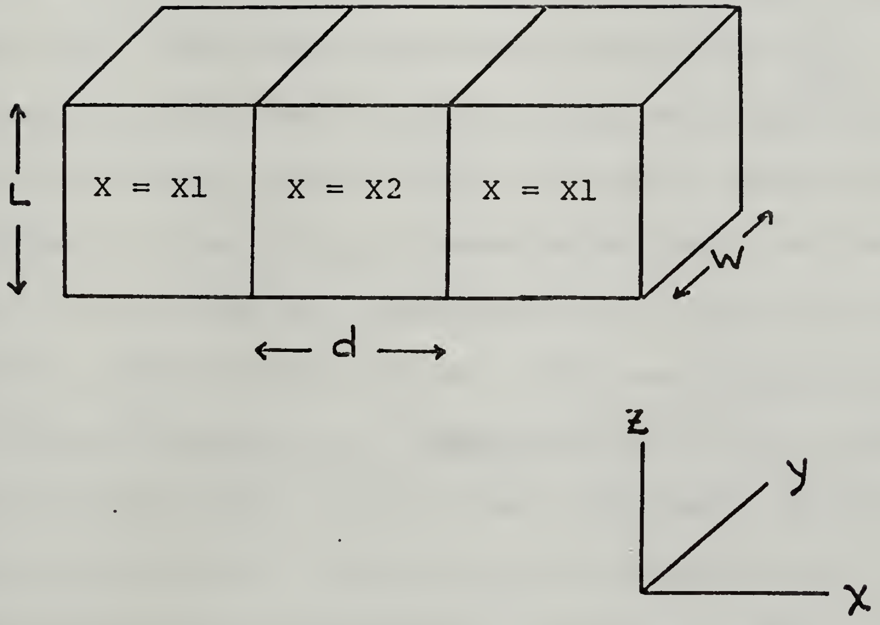

Figure 3.2 Dimension Characteristics of Samples

transitions and assumes that the injected carriers in a semiconductor laser can be approximated by a two discreet level system. The derivation of optical gain will not be repeated here. The final result is

$$\text{gain}\ (\nu) = \frac{c^2\ \xi\ \eta_{int}\ J}{8\pi\ \nu^2\ q\ d_{rad}\ \Delta\nu}$$

where ν = lasing frequence, $\Delta\nu$ = line width of spontaneous transition, ξ = population inversion factor = $1 - \frac{N_1}{N_2} \cong$ 1 at low temperatures, η_{int} = internal quantum efficiency = fraction of injected carriers which recombine radiatively, q = electronic charge, d_{rad} = penetration depth of the electromagnetic waves from the interface of the junction, and n = effective index of refraction. The theoretical calculation of d is difficult because the electromagnetic wave analysis in a semiconductor laser has not been rigorously solved at all. It should be pointed out that in heterojunction lasers, one of the most important improvements is in the reduction of d .

3. Optical Loss in Semiconductor Laser and Lasing Threshold

The optical loss is described by the parameter α defined by the decay of the radiation intensity as $e^{-\alpha z}$. Lasing will occur when the gain of the radiation in a single pass between the reflectors of the optical cavity is equal to the total loss which includes both the reflection loss at the mirrors and other losses inside the cavity.

$$\left(e^{g_{th}L}\right)\left(R e^{-\alpha L}\right) = 1$$

where R = reflectibity at end mirrors of the cavity, L = length of the optical cavity, and α is the loss constant which includes losses due to free carrier absorptions, internal transitions, and diffractions and scatterings. The last component is most effectively controlled by the presence of the heterojunction. The threshold gain for lasing is therefore:

$$g_{th} = \alpha + \frac{1}{L} \ln\left(\frac{1}{R}\right)$$

which can be used to derive the lasing current threshold

$$J_{th} = \frac{8\pi \nu^2 q\, d_{rad}\, n^2 \Delta\nu}{c^2 \eta_{int}\, \xi} \left[\alpha + \frac{1}{L} \ln\left(\frac{1}{R}\right)\right]$$

α is usually separated into three parts:

$$\alpha = \alpha' + \alpha_{FC} + \alpha_{band}$$

where α' is scattering and diffraction losses through the leaky walls of the waveguide. α_{FC} and α_{band} are losses due to free carrier absorption and interband transition respectively. The calculation of α' requires a theoretical analysis of optical confinement

4. Optical Waveguide Theory of a Semiconductor Laser

Several simplified theories have been made to study the distribution of radiation in a semiconductor laser.

One of the most widely quoted analysis is the three layer dielectric waveguide model of W. Anderson (Ref. 25). His analysis has been expanded by Adams and Cross (Ref. 26), and also by Kressel (Ref. 27), and compared with experiments with fair agreement. Anderson obtained an expression for as

$$\alpha' = \frac{1}{F_1} \quad (\alpha_3 + \alpha_1 F_2)$$

where F_1 and F_2 have been numerically solved and presented as a function of normalized cavity width

$$D = \frac{2\pi d}{\lambda_0} \sqrt{n_2^2 - n_1^2}$$

for different values of refractive index difference. α_1 and α_3 are the absorption coefficients at the lasing wavelength in regions 3 and 1 respectively. Anderson also calculated the confinement of the radiation on both sides of the active region by assuming that TE and TM waves exist in the laser. He made the following drastic assumptions in the field distribution.

Assuming that the propagating TE modes are described by

$$E_1 = E_{01}\, e^{j\gamma_1 x}\, e^{j(\beta z + \omega t)} \qquad x \leq -\frac{d}{2}$$

$$E_2 = E_{02} \cos(\gamma_2 x + \phi)\, e^{j(\beta z + \omega t)} \qquad |x| \leq \frac{d}{2}$$

$$E_3 = E_{03}\, e^{-j\gamma_2 x}\, e^{j(\beta z + \omega t)} \qquad x \geq \frac{d}{2}$$

γ_1 , γ_2, and γ_3 are the transverse wavenumbers. These parameters together with ϕ and β can be solved by the following equations.

$$\gamma_i^2 + \beta^2 - \frac{\epsilon_i \omega^2}{c^2} = 0 \qquad i = 1,2,3$$

$$\tan \gamma_2 d = j \, \frac{\dfrac{\gamma_3}{\gamma_2} + \dfrac{\gamma_1}{\gamma_2}}{1 + \dfrac{\gamma_3}{\gamma_2}\,\dfrac{\gamma_1}{\gamma_2}}$$

$$2\phi = \tan^{-1}\left(\frac{\mathcal{R}(\gamma_1)}{\gamma_2}\right) - \tan^{-1}\left(\frac{\mathcal{R}(\gamma_3)}{\gamma_2}\right) + m\pi$$

where m is an integer. Once γ_1, γ_2, and γ_3 are determined, the penetration of radiation across the active region is assumed to be

$$d_{rad} = d + \frac{1}{\mathcal{R}e(\gamma_1)} + \frac{1}{\mathcal{R}e(\gamma_3)}$$

from which the threshold current can be calculated. There are two other laser performance parameters which can also be calculated.

The first one is the external differential quantum efficiency

$$\eta_{ext} = \frac{\eta_{int}}{1 + \dfrac{\alpha L}{\ln\left(\frac{1}{R}\right)}}$$

The other one is the power output as a function of bias current j

$$P = \frac{\eta_{ext}}{\eta_{int}} \, \eta_{int} \, (J - J_{th}) LWV_A$$

where L = laser length, W = laser width, and V_A = applied bias voltage.

B. THEORETICAL CALCULATION OF A DOUBLE HETEROJUNCTION $Pb_{1-x}Sn_xTe$ LASER

1. Introduction

A $Pb_{1-x}Sn_xTe$ double heterojunction (DH) laser was analyzed. The active region #2 was selected as x = 0.20. The outer regions #1 and #3 are assumed to be the same and have larger energy gaps than the active region. In other words, their Sn composition x is less than 0.20. The simplified theory described in section A was used to analyze the effects on a DH $Pb_{1-x}Sn_xTe$ laser properties using the following factors

a. Active region thickness d

b. Alloy composition of the outer regions

c. Cavity length L

Before the numerical results are presented, the equations used for these calculations will be summarized.

The optical confinement can be calculated by first determining the transverse wavenumbers

$$\gamma_1 = \gamma_3 = -jb$$

γ_2 is real

for the lowest order TE mode, i.e., $m = 0$, $\phi = 0$. γ_1, γ_2 and β can be solved from the simultaneous equations

$$\tan \gamma_2 d = \frac{2\, b/\gamma_2}{1 - (b/\gamma_2)^2}$$

$$\gamma_2^2 + b^2 = (\epsilon_2 - \epsilon_1)\left(\frac{2\pi}{\lambda_0}\right)^2$$

The radiation penetration width is

$$d_{rad} = d + \frac{2}{\gamma_1}$$

The tranverse field distribution is given by

$$E_3 = A\, e^{-bx}$$

$$E_2 = B \cos\,(\gamma_2 x)$$

The optical loss coefficient α is calculated in the following ways

(a). α_{band} is neglected in comparison with α_{FC}.

(b). $\alpha_{FC} = \dfrac{N\, q^3\, \lambda_0^3}{4\pi^2 n_2 c^3 \epsilon_0 \mu_c {m_c^*}^2}$

where λ_0 = the lasing wavelength, n_2 = refractive index in the active region, μ_c = mobility, m_c^* = conductivity effective mass, and N = carrier concentration in the outer regions.

(c). α_1 and α_3 will be selected from experimental absorption data. α' = scattering and diffraction loss will be

determined from Anderson's computer result. $F_2 = 1$ for the symmetrical case

$$\therefore \quad \alpha = \frac{2\alpha_1}{F_1} + \alpha_{FC}$$

The lasing threshold current density is calculated by

$$j_{th} = \frac{8\pi q d_{rad}\, n_2^2\, \Delta\nu}{\eta_{int}\, \lambda_o^2} \left[\alpha + \frac{1}{L}\ \ln\left(\frac{1}{R}\right)\right]$$

The other two laser performance parameters η_{ext}/η_{int} and P are then calculated.

2. Numerical Parameters for $Pb_{1-x}Sn_xTe$

a. The refractive index n of $Pb_{1-x}Sn_xTe$ at 80°K is shown in Figure 3.5. It can be seen that n has a peak at the photon energy near the energy gap which is expected in a direct gap semiconductor. The peak n can be approximated by

$$n = 6.32 + 2.61x$$

b. The energy gap of $Pb_{1-x}Sn_xTe$ is given by

$$E_g(x, 77^\circ K) = 0.22 - 0.5x$$

c. The conductivity effective mass can be determined from the experimental density of state effective mass of $Pb_{1-x}Sn_xTe$ shown in Figure 3.9 by the following relationships

$$m_d^* = (K)^{1/3} m_T$$

where K = anisotropy effective mass ratio = 10

$$m_d^* = \frac{3m_T}{2 + \frac{1}{K}}$$

d. $\Delta\nu$ is chosen to be 5000 GHz

e. η_{int} is chosen to be 0.1

f. L varied from 0.001 cm to .6 cm (10 to 600 μm)

g. $R = \left(\frac{n_{2-1}}{n_{2+1}}\right)^2$

h. The value of α_1 was selected as 40 from experimental absorption data (Ref. 24), Figure. 3.11.

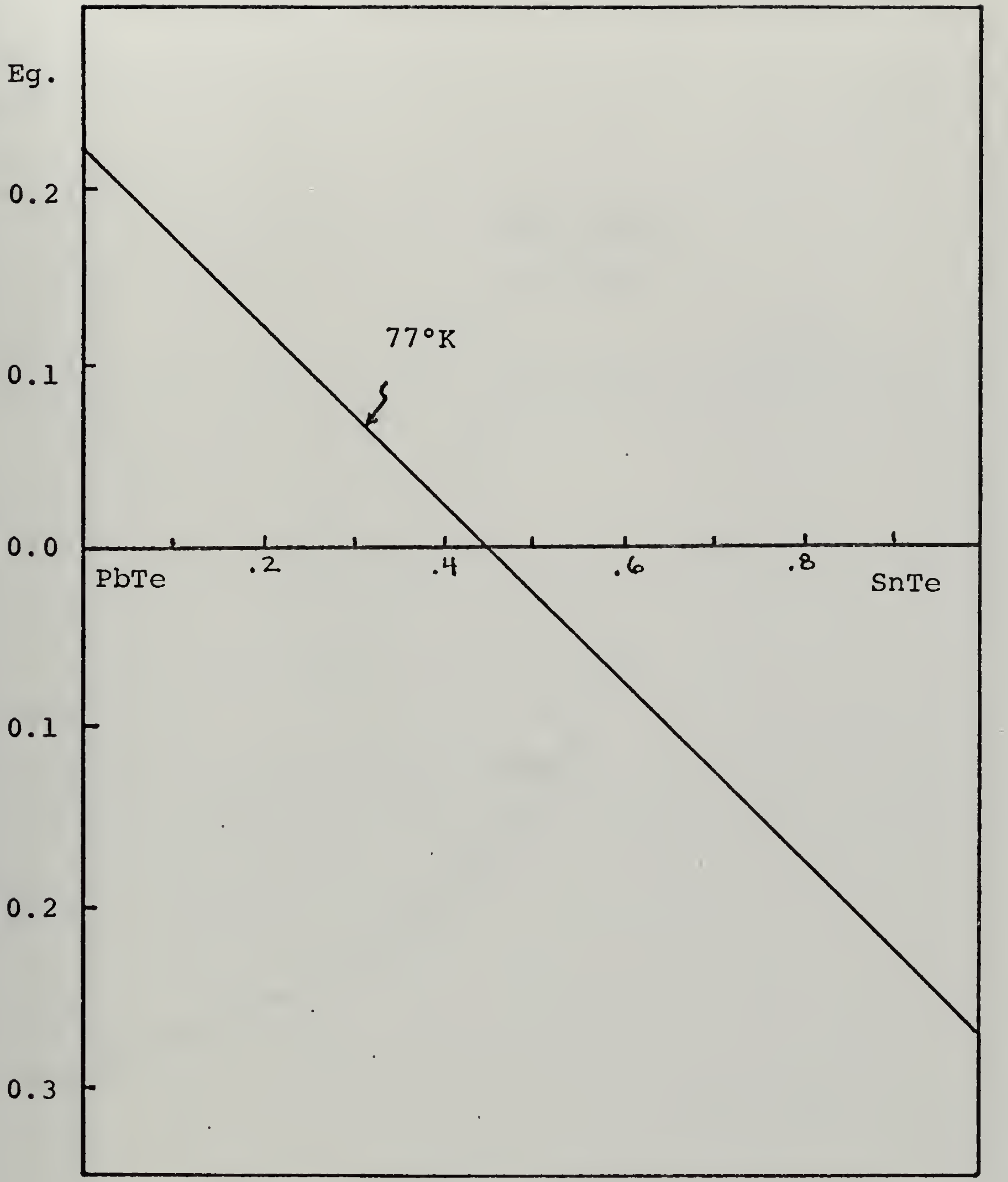

Figure 3.3 Energy Gap (eV) vs. Composition x

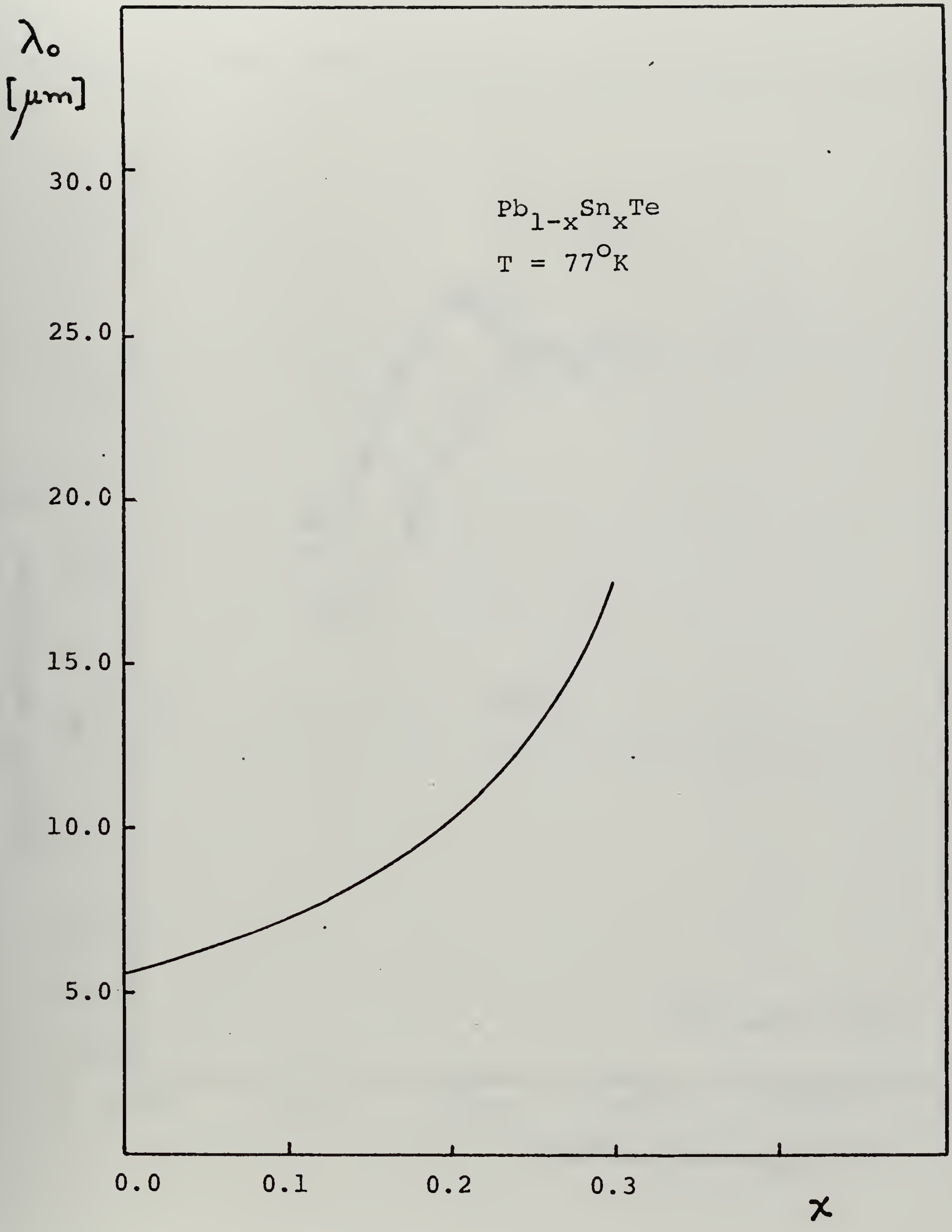

Figure 3.4 λ_o versus Composition x

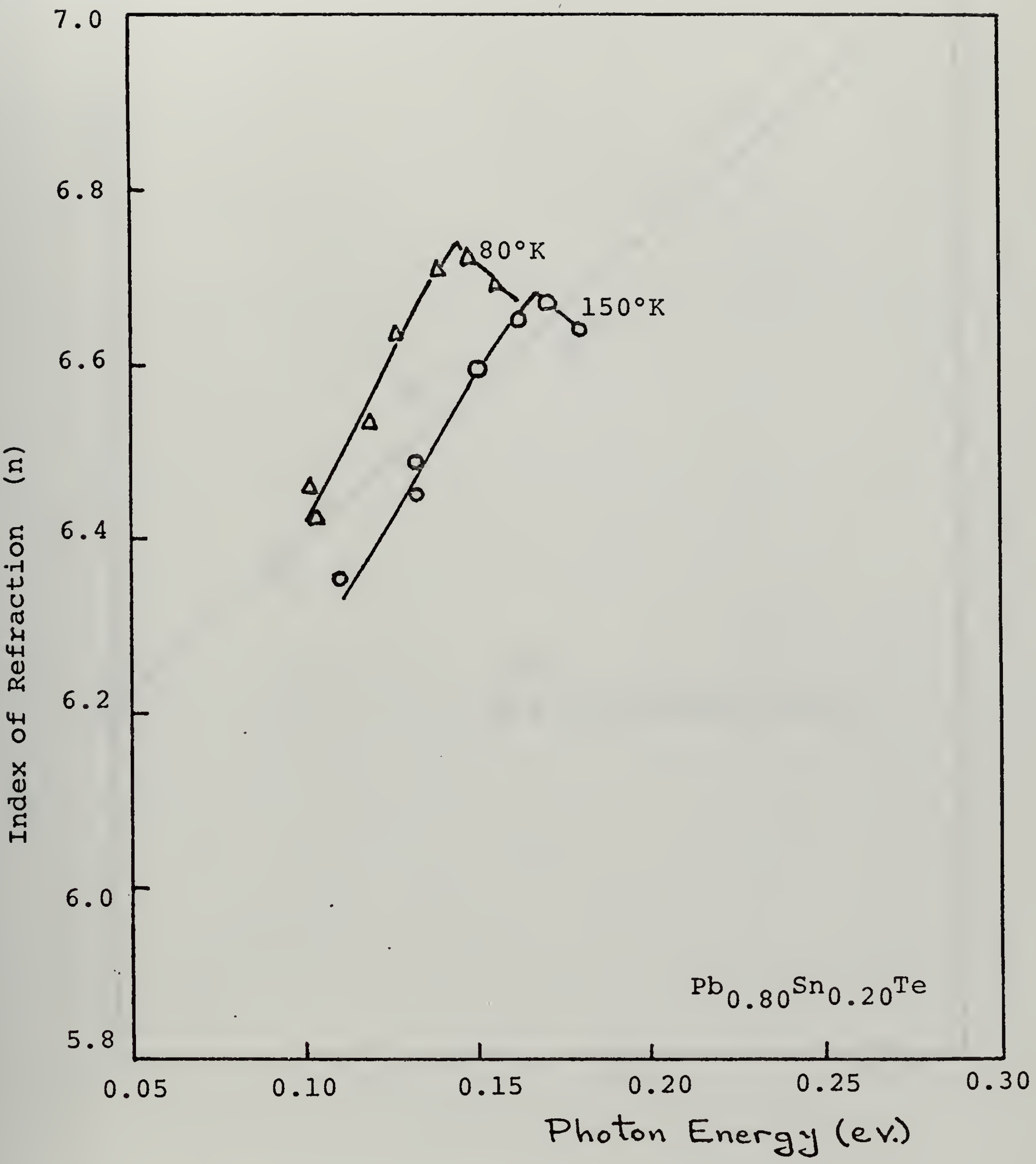

Figure 3.5 Photon Energy (ev)

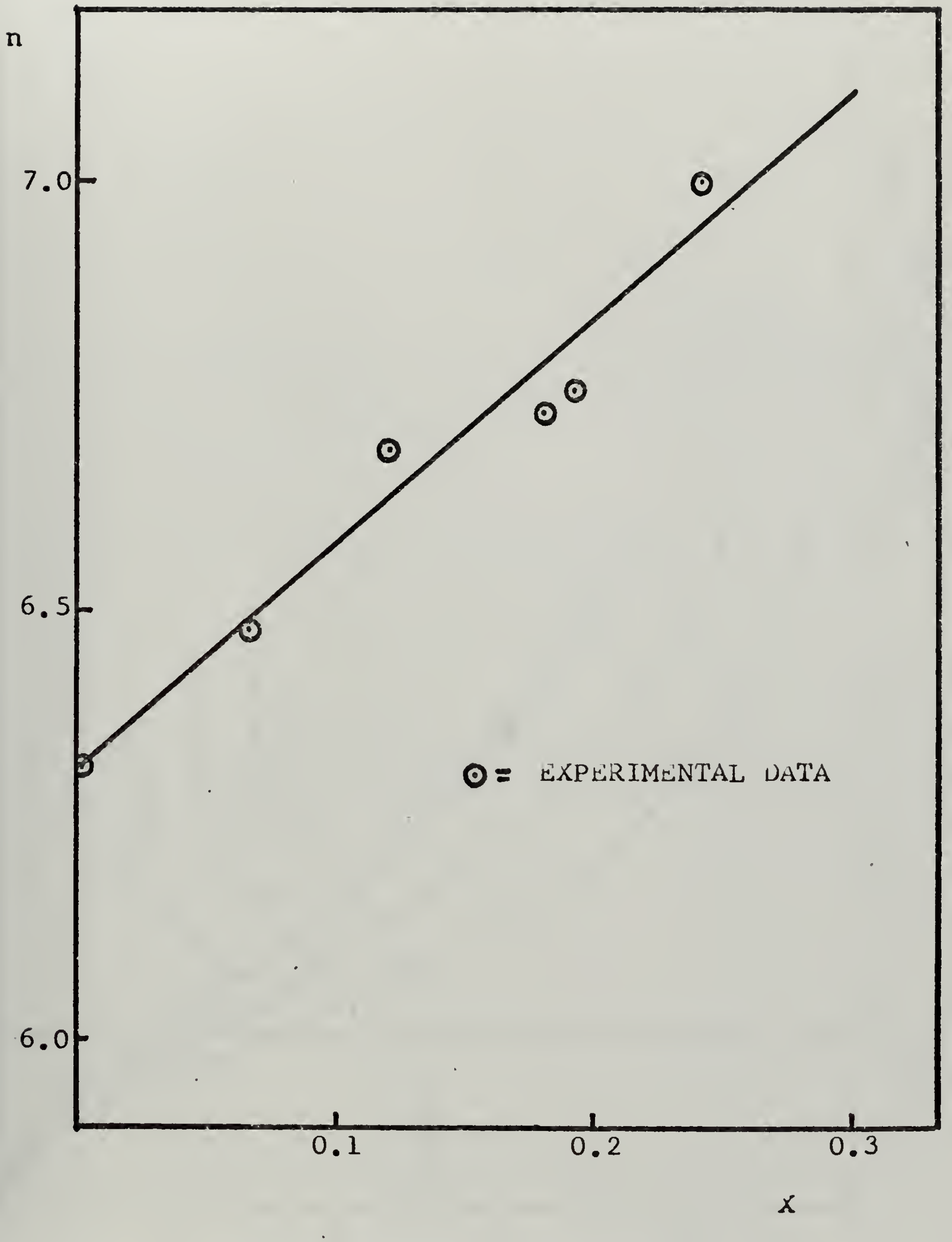

Reflection coeff. vs. composition

Fig. 3. 6

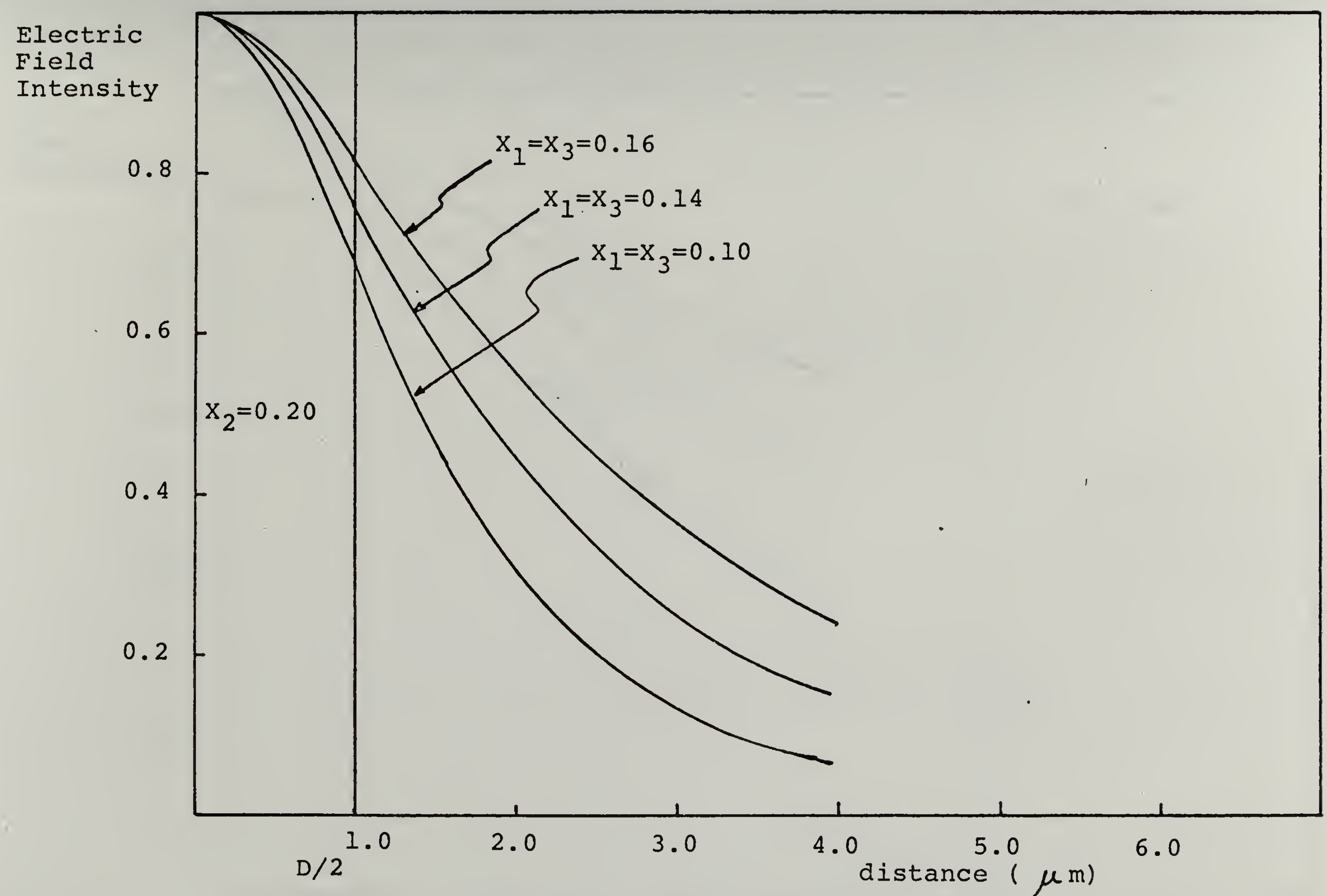

Figure 3.7 Electrical Field Intensity for $d=2\mu m$

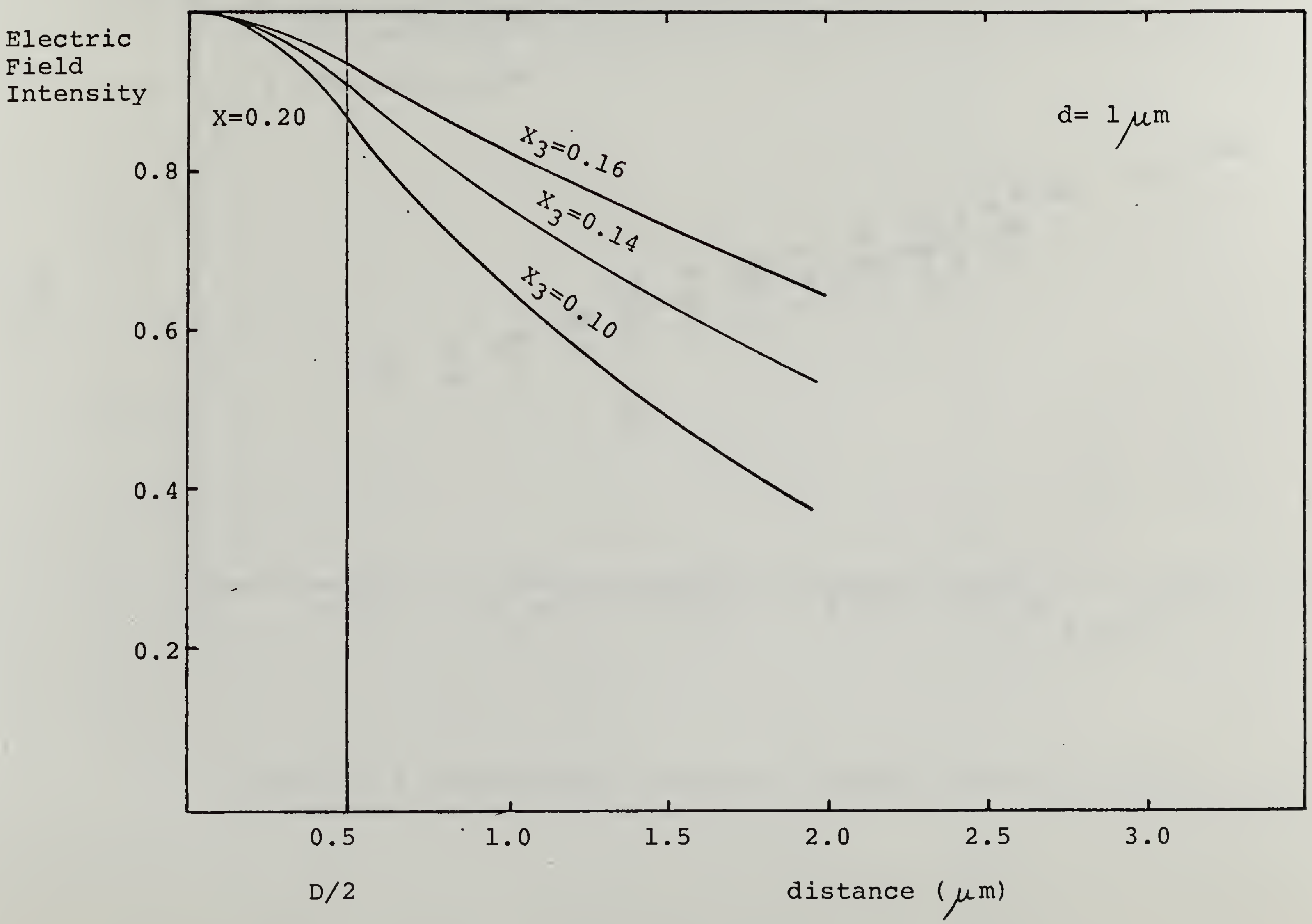

Figure 3.8 Electrical Field Intensity for d=1μm

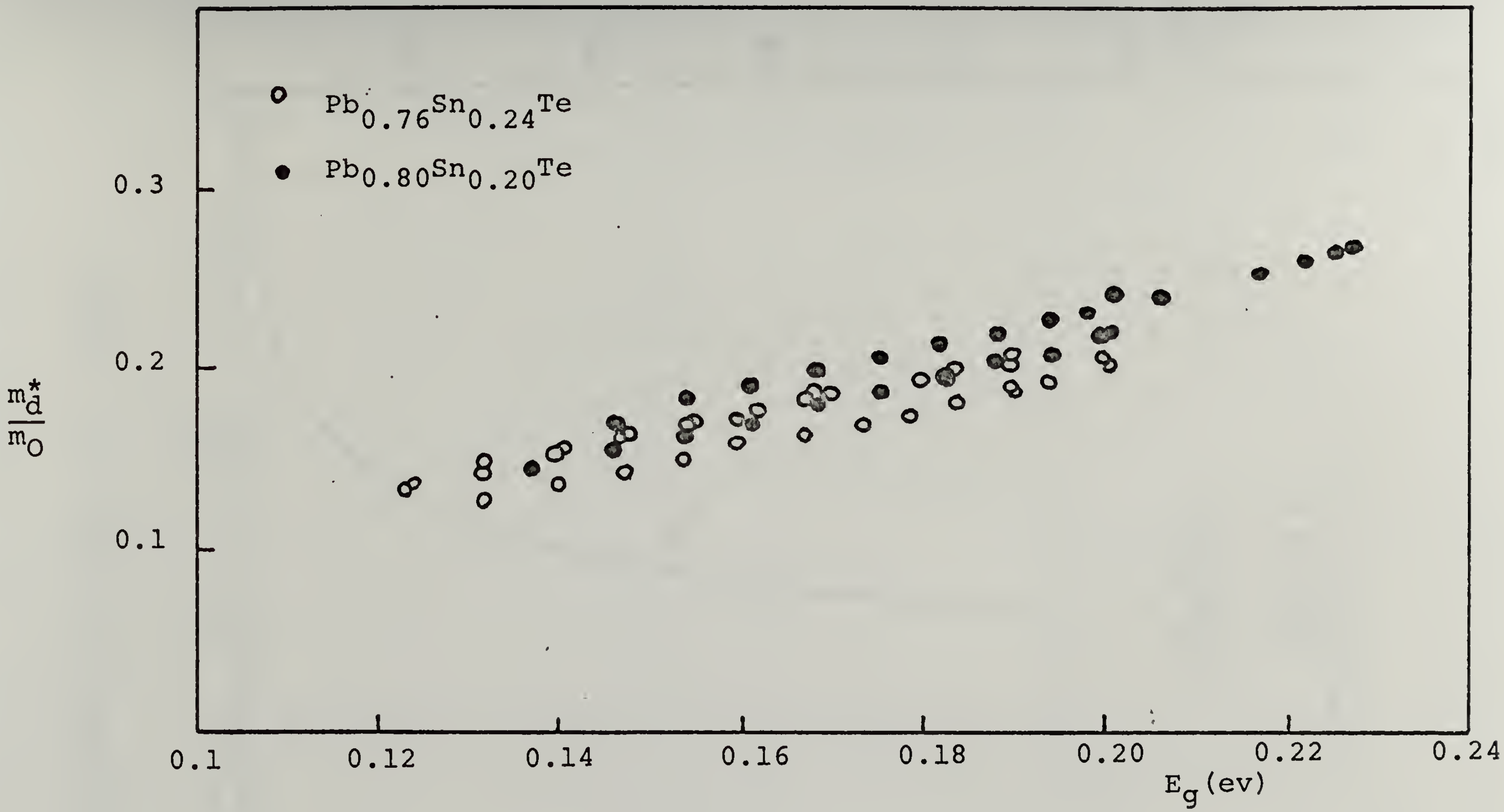

Figure 3.9 Experimental Results of md^*/m_o versus E_g

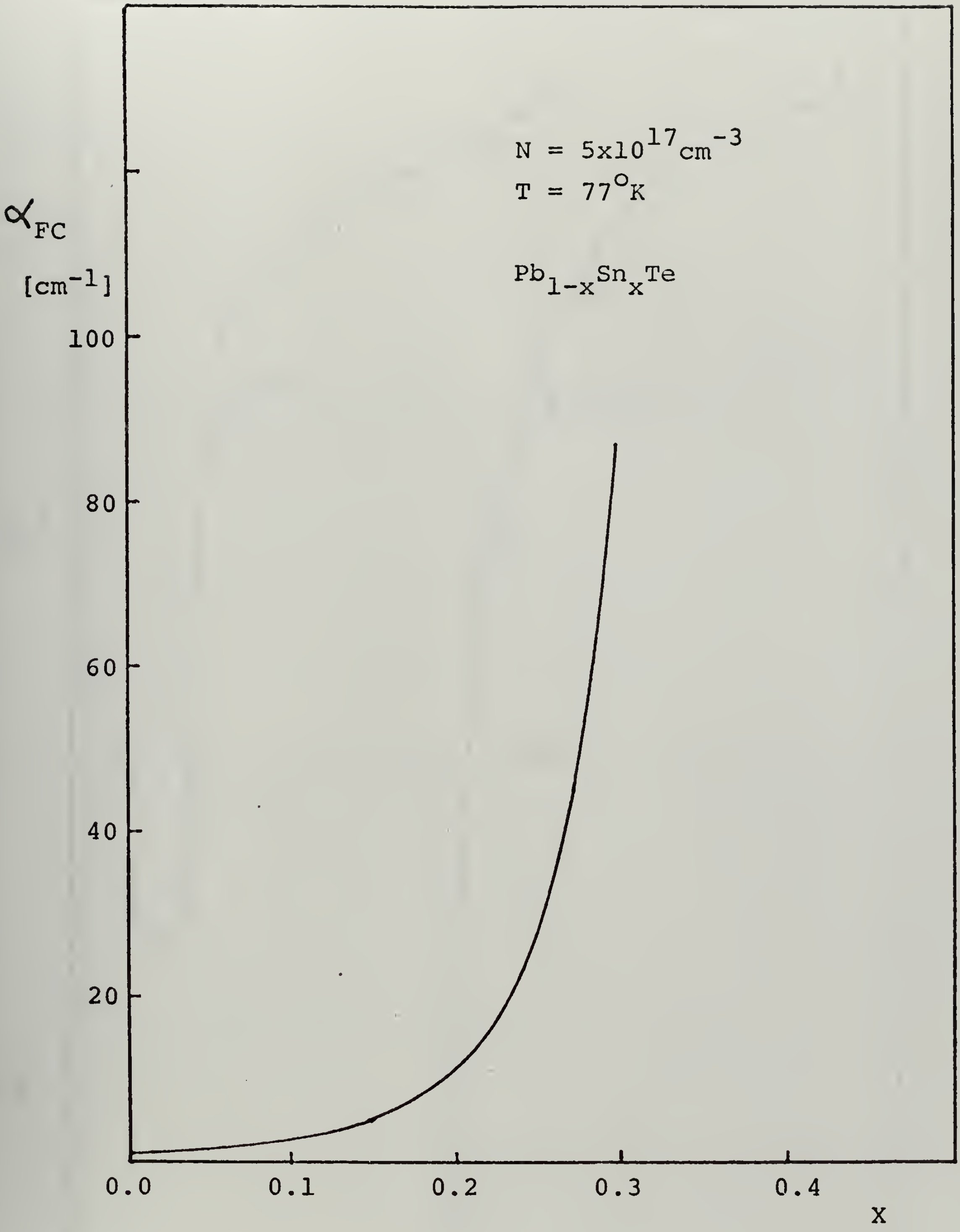

Figure 3.10 α FC vs. Composition

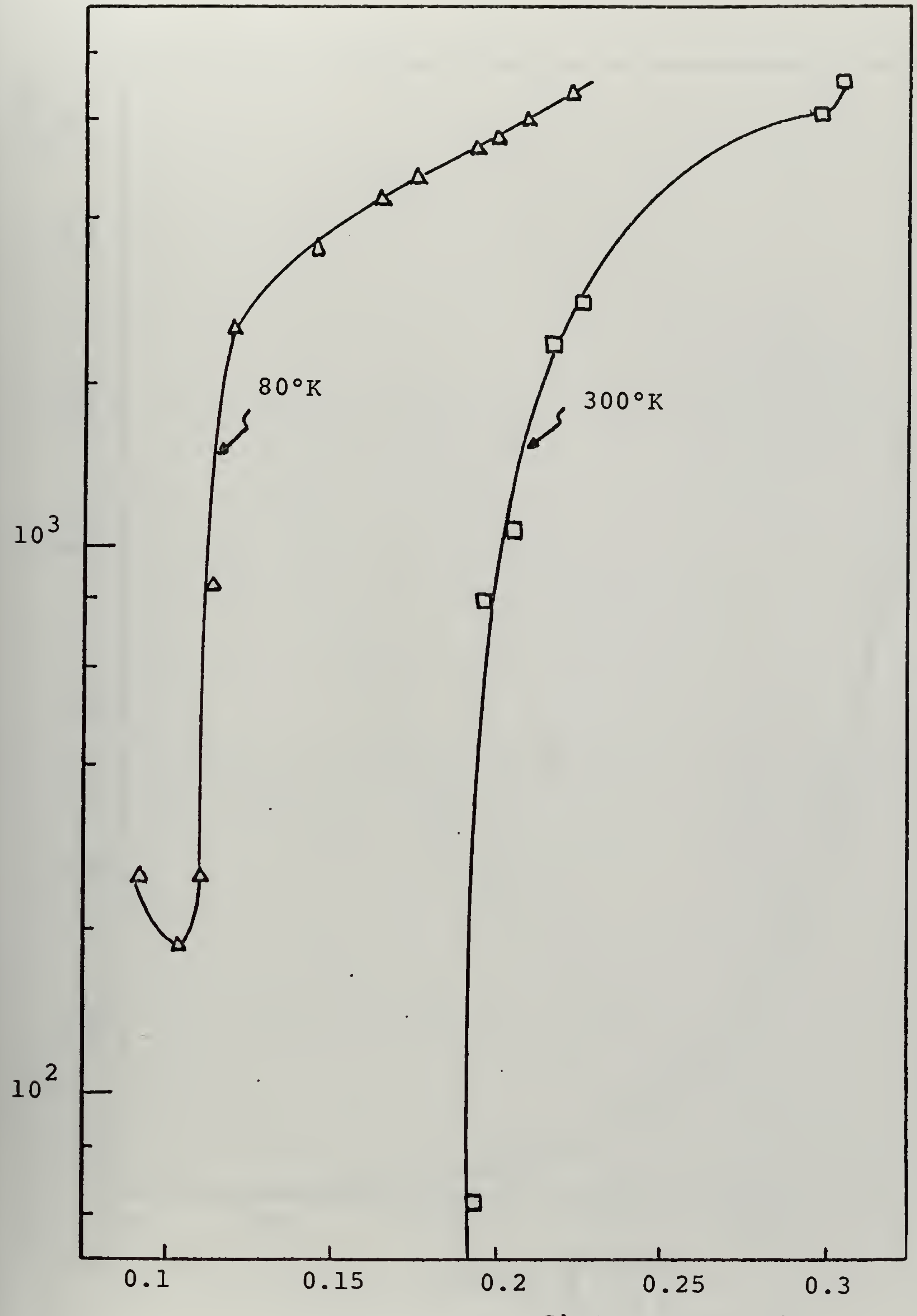

Figure 3.11 The Absorption Coeff. for $Pb_{1-x}Sn_xTe$ Alloy

X=0.20

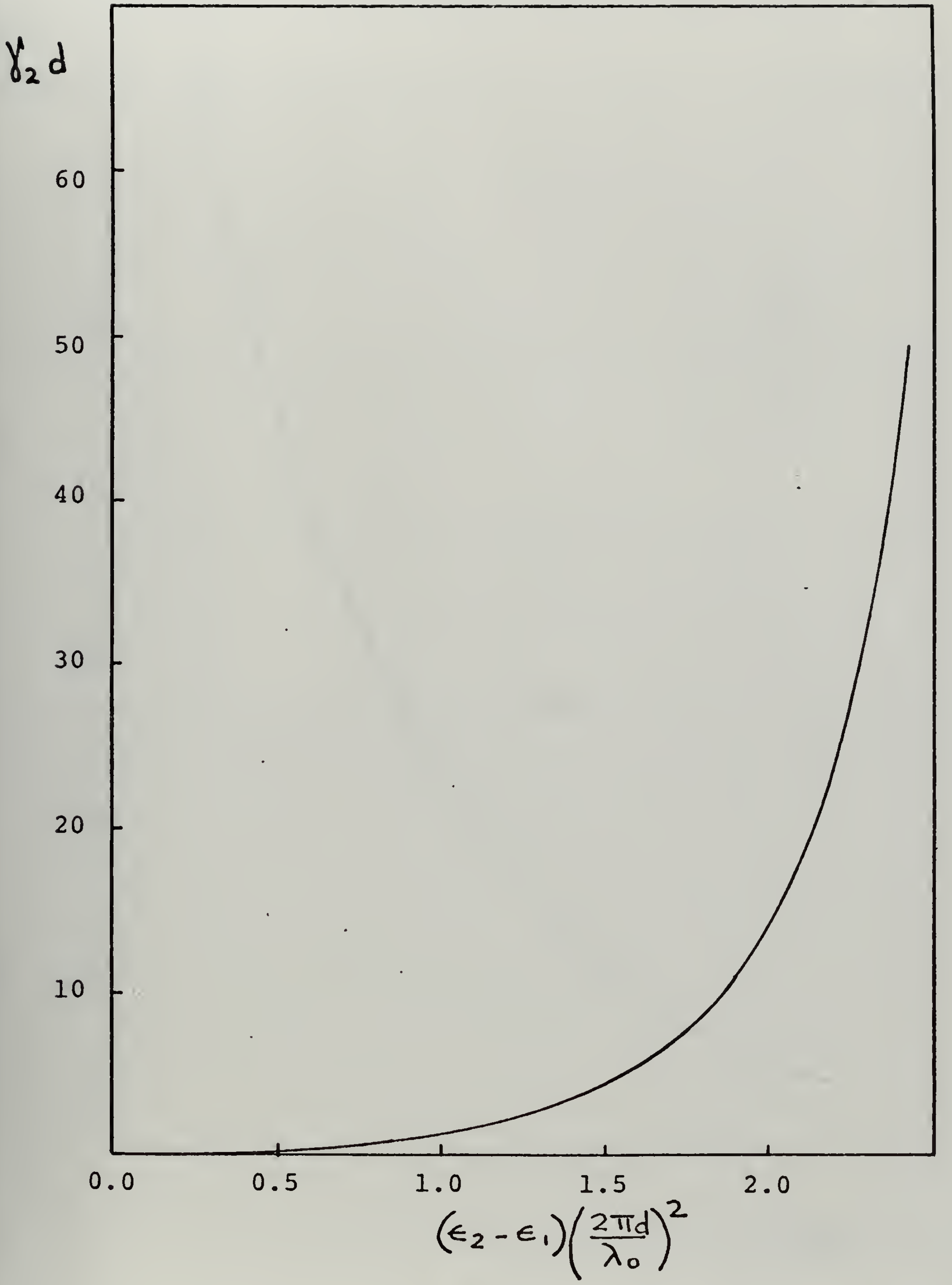

Figure 3.12 $\gamma_2 d$ versus $(\epsilon_2 - \epsilon_1)\left(\frac{2\pi d}{\lambda_0}\right)^2$

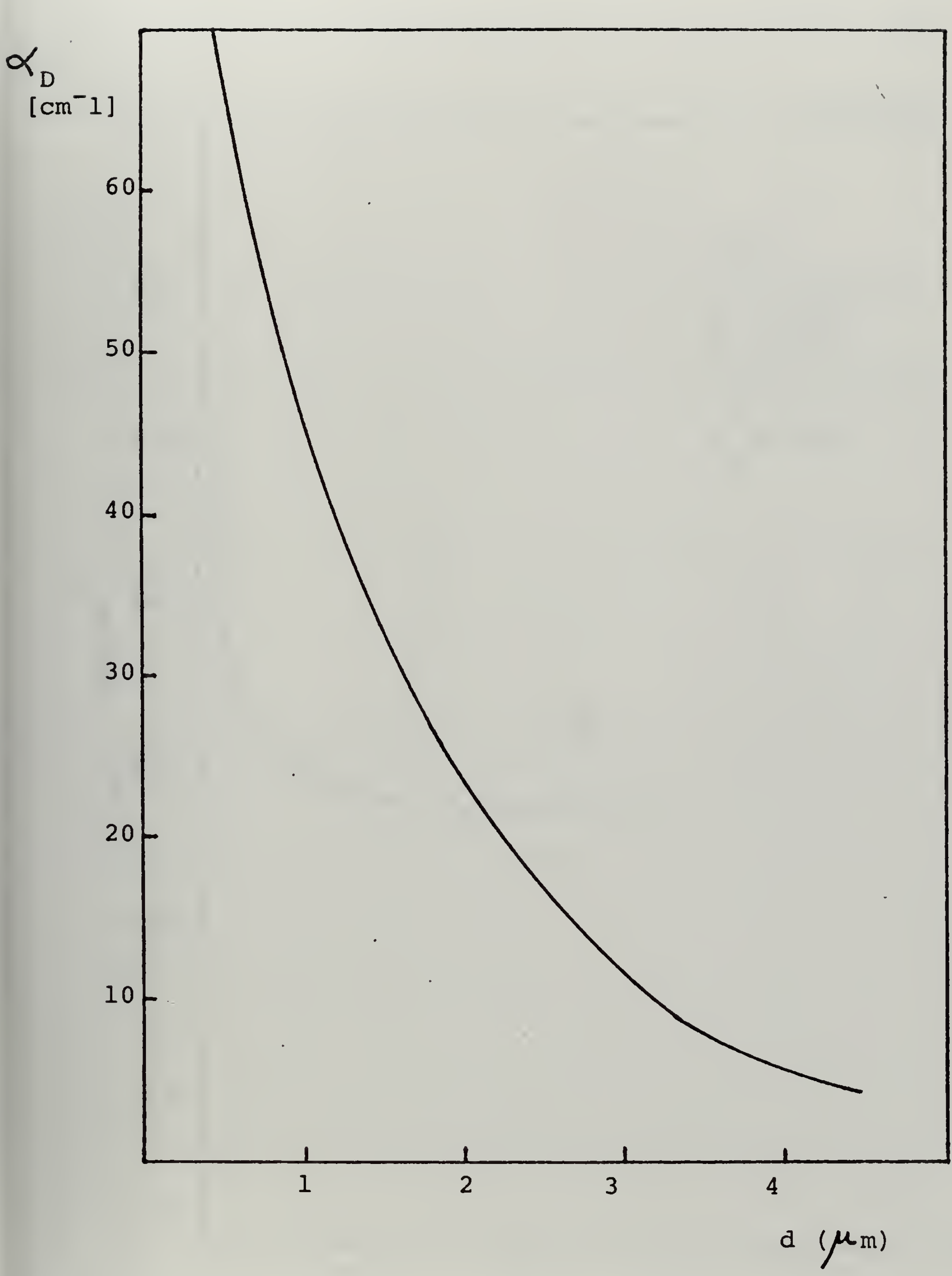

α_D versus d

Figure 3.13

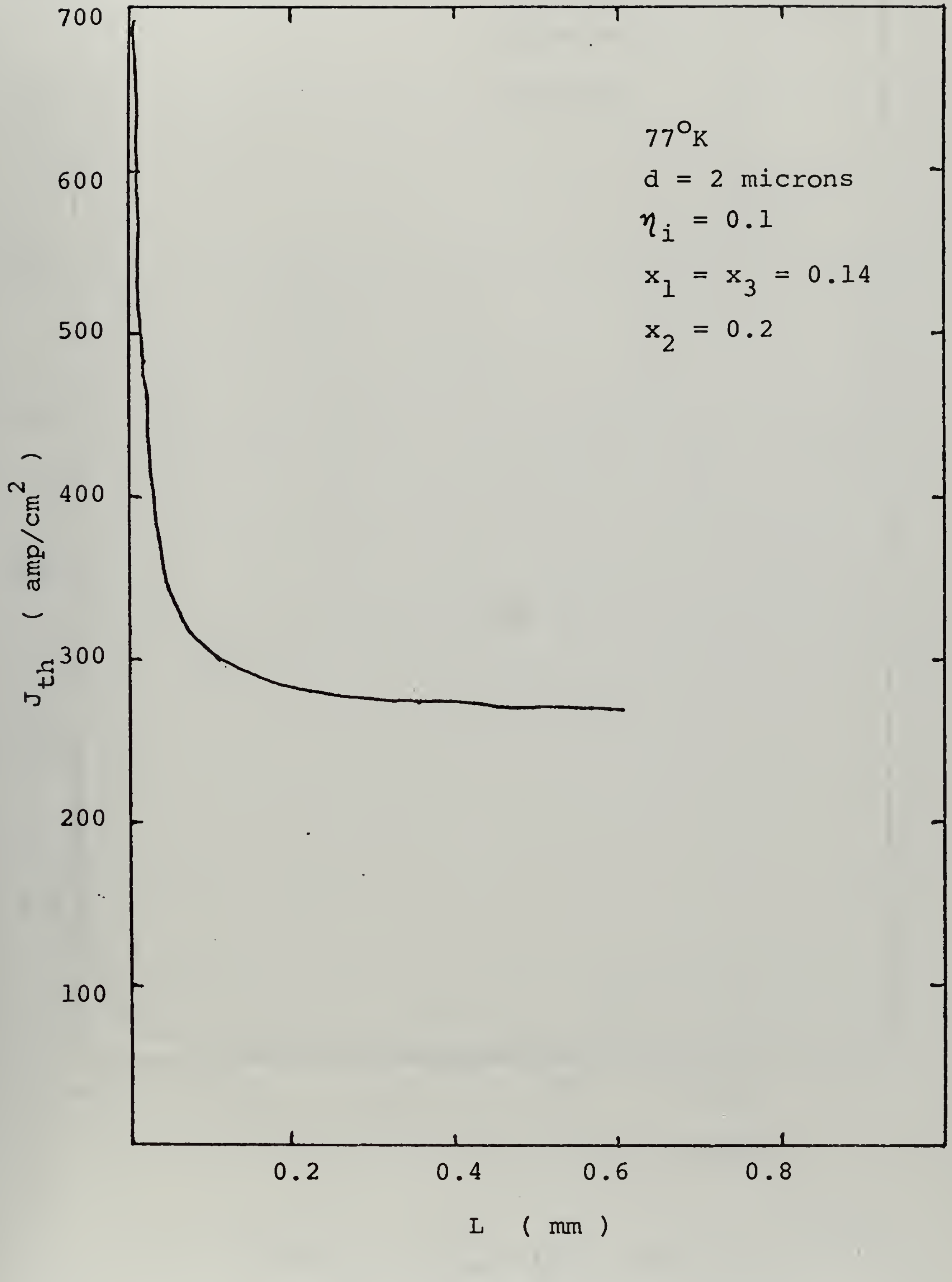

Figure 3.14 J_{th} versus L

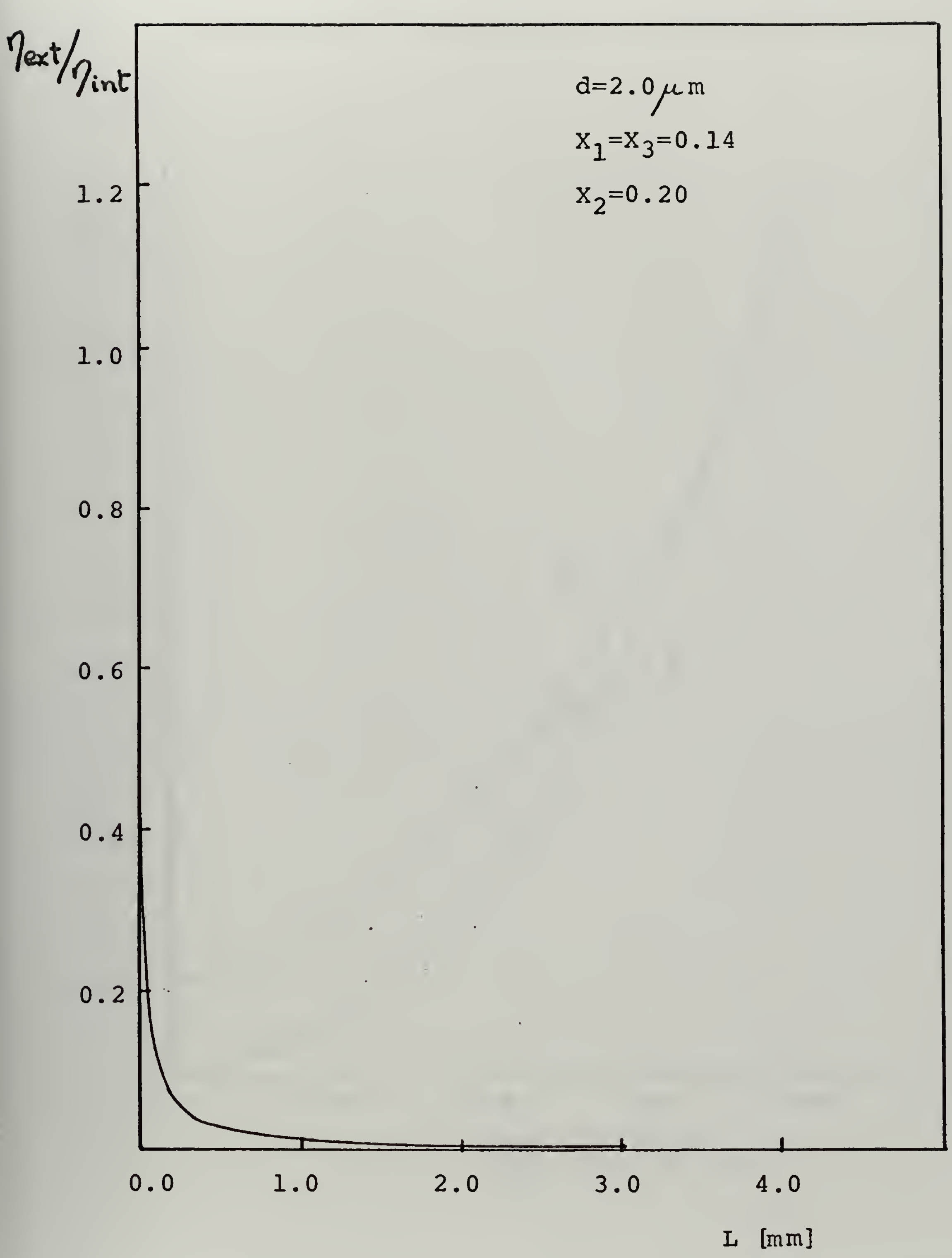

Figure 3.15 η_{ext}/η_{int} versus L

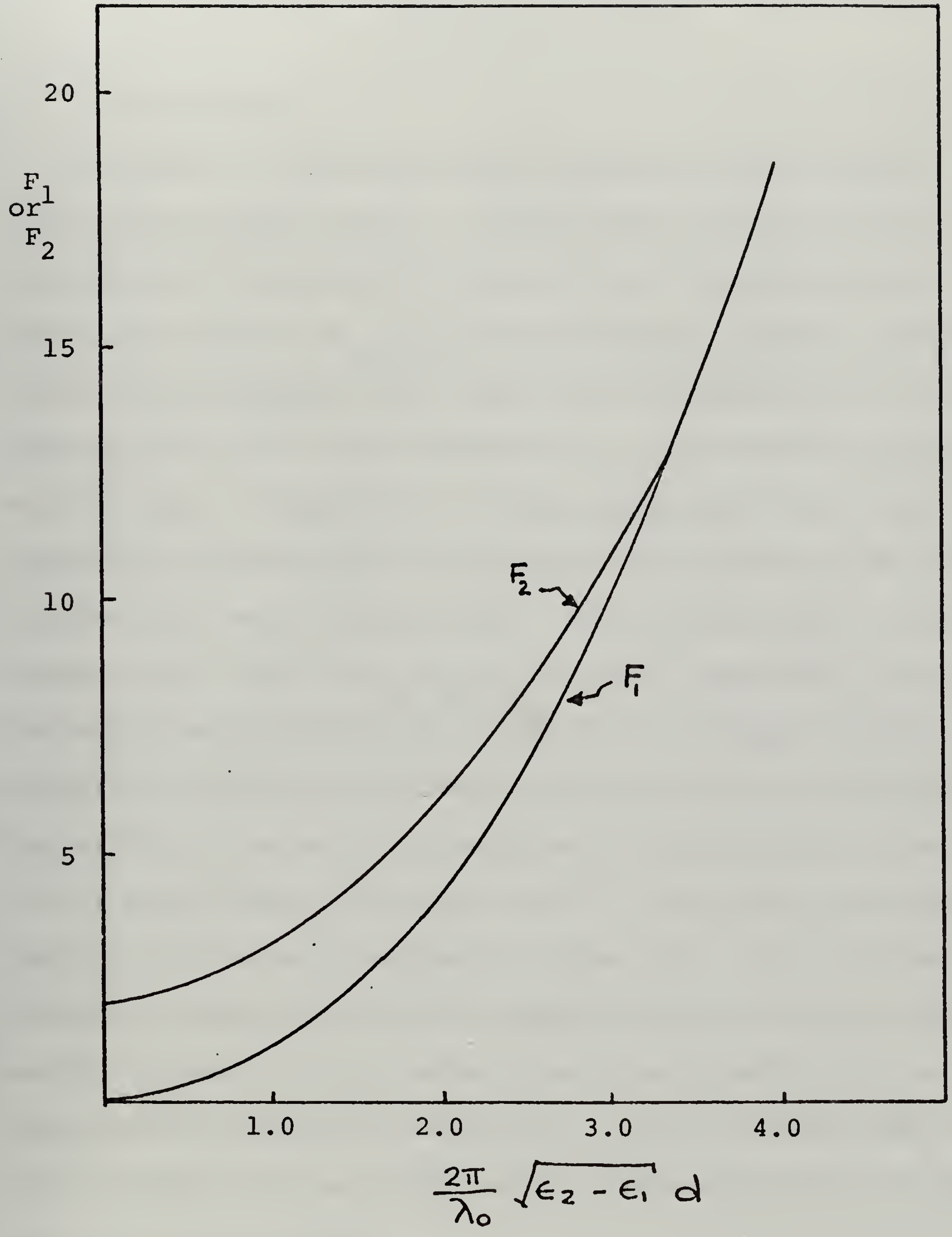

Figure 3.16 F and G Parameters versus $(2\pi/\lambda_0)\sqrt{\epsilon_2-\epsilon_1}\,d$

IV. EXPERIMENTAL STUDY OF SINGLE HETEROJUNCTION $Pb_{1-x}Sn_xTe$ DIODES

A. INTRODUCTION

Although 3-5 heterojunction devices did not become practically useful until a liquid phase epitaxy process was successfully developed for fabricating 3-5 alloy heterojunctions such as $Ga_{1-x}Al_xAs$-GaAs diodes. However, there are supporting evidences that luminescence properties in 4-6 compound and alloy semiconductors are not affected by crystal defects as badly as in other semiconductors. The first supporting evidence was the successful development of Schottby barrier $Pb_{1-x}Sn_xTe$ laser diode. It indicated that the surface state at the metal $Pb_{1-x}Sn_xTe$ interface apparently did not introduce enough irradiative defects to prevent lasing. Recently, photovoltaic detectors using PbTe thin films were reported to have detector performance approaching state of art of bulk crystal detectors [28]. PbTe thin film Schottby barrier diodes were reported to lase also. All of these evidences suggested that 4-6 semiconductors tolerate more crystal defects without deteriorate their photoelectric and luminescence properties severely. It was decided that a thin film process will be developed for fabricating $Pb_{1-x}Sn_xTe$ heterojunction diodes.

To initiate this research, a single heterojunction diode was planned instead of the double heterojunction diodes because there has not been any previous research reported

and much needs to be done to simply establish the feasibility of such a process in fabricating good quality heterojunction $Pb_{1-x}Sn_xTe$ diodes.

In the past three years or so, several groups have been actively developing thin film process to deposit thin films of 4-6 alloy semiconductors. Except the flash evaporation method which was once developed by this research group [29], these groups all use in one way or another, variations of a one boat evaporation method. The source materials used are mostly stoichiometric $pb_{1-x}Sn_xTe$ alloys although one group uses PbTe and SnTe compounds. Most of the films prepared were p type with carrier concentration typically in the high 10^{17} to low 10^{18} cm^{-3} range. An isothermal annealing technique has been developed to control both the carrier type and carrier concentration. Both n and p type semiconductor can be obtained with carrier concentration as low as mid 10^{15} cm^{-3} by properly selecting the annealing temperature and time. Since the annealing temperature varies considerably with the composition, it is felt that the isothermal annealing technique will not be suitable for a heterojunction diode in which $Pb_{1-x}Sn_xTe$ alloys of two compositions are present.

In order to fabricate a p-n heterojunction without using the isothermal annealing method to obtain the n layer, the first task of this thesis is to develop a deposition process which can produce n type $Pb_{1-x}Sn_xTe$ films consistently and reproducibly. The second task is to fabricate a diode of small enough size out of this heterojunction structure.

B. DEPOSITION AND CHARACTERIZATION OF FILMS

1. Preparation of Source Materials

For p type layer, deposition stoichiometric $Pb_{0.86}Sn_{0.14}Te$ alloy were used as source materials. For n type layer, metal rich $(Pb_{0.80}Sn_{0.20})_{1+\delta}Te$ were prepared by melting properly weighted metal rich Pb, Sn and Te elements in a vacuum sealed quartz ampoules at 1100°C for 18 hours and rapidly quenched in water in order to prevent excessive precipitation. The alloy ingots were then crushed into small chunks for use in deposition.

2. Deposition of Films

The procedure employed was the one-boat evaporation technique, or Knudsen method. Several small pieces of the material to be deposited were placed in a close graphite container with a hole of about 1/16 of an inch on the top cover that allowed the evaporation of the material. The cover with the hole on it was also made of graphite. The heater used for heating the boat was a tungsten wil, and the whole system was shielded with a molybdenum sheet in order to decrease the heat losses. A distance of about 6 inches separates the boat from the substrate holder, and a shutter separate both system in order to control the deposition. After the vacuum system is evacuated up to the range of low 10^{-6} torr, the substrate holder was heated at 270°C with a thermocouple automatic controller. Same method was used in order to keep a temperature of 765°C in the boat. After the

system started to evaporate, a delay time of about 5 minutes was made before opening the shutter, allowing in this way that all the possible impurities were deposited on the shutter and not on the substrate. The rate of deposition was fairly in the range of 10 µm per hour and the time varied from half an hour to one hour. After the time presupested was over, the shutter was closed, and a time of about 4 hours was allowed for woling the substrate to room temperature. After that, the normal pressure was restored and the samples were removed, inspected, and stored.

The thin films deposited showed good adherence to the substrate and smooth surface, and their thickness varied from 0.6 to 10 µm, depending on the deposition times.

The selection of the KCL substrate was made for the following characteristics: a) good adherence of thin films, b) 100 crystal orientation, c) easy for cleaning and d) disolubility in water. All these characteristics are important for the heterojunction diode fabrication.

3. Metallurgical Evaluation

The films were tested in order to obtain information of thickness, crystal structure, orientation and composition.

The thickness were obtained from a Perking-Elmer spectrophotrem taking measurements of the transmittance versus wavelength. The difference between peaks was measured and using the relationship for $Pb_{1-x}Sn_xTe$, $t=\frac{1000\,\Delta m}{\Delta\gamma}$, where $\Delta\gamma$ is the difference in wavelength and Δm the difference of peaks using in the measurement.

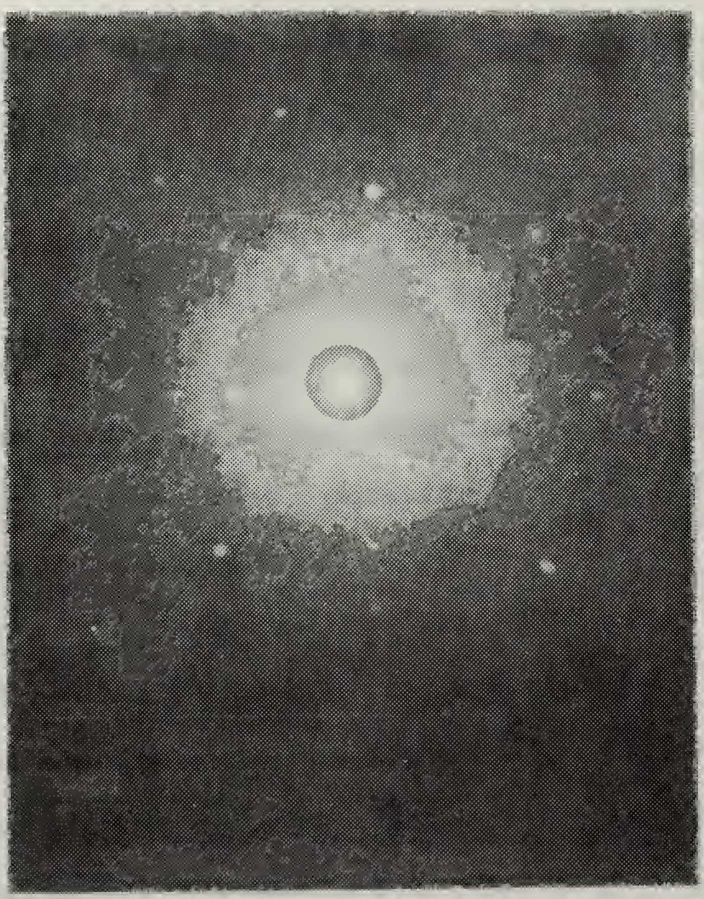

FIGURE 4.1 LAUE-PICTURE OF SOURCE MATERIAL A.- INDICATING SINGLE CRYSTAL STRUCTURE.

[illegible]

The crystal structure was tested using the x-ray lane picture technique, where all the thin-films showed bright spots and ausence of Delaye rings, indicating single crystal structure.

The orientation and composition were obtained with a Norelco x-ray diffractometer using a copper target. The crystal orientation was obtained using the angular position of the intensity peaks and the composition from the characteristics of the peaks, with the frequency. The results indicate the agreement of the 100 orientation and the valves of the source material employed.

4. Electrical Measurements

Hall coefficients and conductivity were carried out from 90°K to 300°K. From the temperature variation of the electrical data, the carrier scattering mechanism as well as the influence of the substrates can be revealed. A constant current of 1mA was passed through the sample. The Hall sample was mounted in a cold finger of a liquid Nitrogen dewar. The electrical contacts were made to the olunic gold pads already evaporated on the sample and soldered with silver epoxy to copper wire. The contacts in the cold finger were made soldering these wires with Indiun alloy number eight. A thermocouple device sumiuistrate data for the temperature. An x-y recorder was used to record the output desired versus temperature. The system was keeping in vacuum of about 20μ during the measurements.

COLD FINGER USED FOR SAMPLE CONNECTIONS
FOR HALL MEASUREMENTS

EQUIPMENT USED FOR HALL MEASUREMENTS

Figure 4.2 Hall Measurements Devices Used

The conducting voltage was obtained from two sequential pins, biasing the sample with a current of 1ma., and reading the voltage drop across a portion of the sample from room temperature to 90°K.

The Hall measurement was made measuring the voltage across the sample from 90°K to room temperature applying on and off a magnetic field of 5000 gauss. Using the data sumiuistrated for these measurements, the carrier concentration and the movility were calculated. The results of these measurements are shown in table II.

C. DEPOSITION OF N TYPE FILMS

1. Preparation of Metal Rich Source Materials

Thin films prepared from stoichiometric alloy sources by the one boat evaporation method have always been p type with carrier concentration typically in the low 10^{18} cm^{-3} range. If n type films are needed, an isothermal annealing technique can be used to change the p type semiconductor to n type and also to lower the concentration. In this research, a different approach was made by using metal rich $(Pb_{1-x}Sn_x)_{1+\delta}Te$ alloy as source material. The idea behind this method is that excess Pb/Sn will introduce donors and give n type films.

2. Deposition of n-Type Films

In this research, varying from 0104 to 0.0006 were used as shown in Table IV-1. They were deposited on cleaved (100) KCL substrates. X-ray measurements indicated that the films were all single crystal (100) oriented.

TABLE IV-I

COMPOSITION OF SOURCE MATERIAL $(Pb_{1-x}Sn_x)_y Te$

SAMPLE	X	Y
A	0.20001	1.0047
B	0.19999	1.0028
C	0.20000	1.0010
D	0.20000	1.0006
E	0.20000	1.0020
F	0.20000	1.0030
G	0.19999	1.0040
H	0.20000	1.0060
I	0.20000	1.4000

TABLE IV-2

ELECTRICAL CHARACTERISTICS

SAMPLE	THICKNESS (μm)	CARRIER CONCENTRATION (cm^{-3})	MOBILITY (cm^2/v-sec)	CARRIER TYPE
ST-20-J-A-2-4	2.55	$2.8 x 10^{17}$	6,400	n
ST-20-J-A-4	0.60	$1.0 x 10^{17}$	4,400	n
ST-20-J-A-2-2	2.55	$1.0 x 10^{18}$	5,900	n
ST-20-J-B-3	3.7	$1.5 x 10^{17}$	3,900	n
ST-20-J-B-4	3.7	$2.6 x 10^{17}$	4,400	n
ST-20-J-B-5	3.7	$1.8 x 10^{17}$	9,500	n
ST-20-J-C-2	8.5	$9.8 x 10^{17}$	13,500	p
ST-20-J-C-5	8.5	$1.0 x 10^{18}$	9,000	p
ST-20-J-D-5	2.65	$3.7 x 10^{17}$	1,000	n
ST-20-J-D-4	2.75	$1.7 x 10^{17}$	2,000	n

SAMPLE	THICKNESS (μm)	CARRIER CONCENTRATION (cm^{-3})	MOBILITY (cm^2/v-sec)	CARRIER TYPE
HT-20-IJ-A-3	4.25	7.8×10^{17}	5,400	n
HT-14-IJ-S-2	8.5	3.3×10^{17}	11,500	p
HT-20-2J-B-2	3.85	3.7×10^{17}	5,400	n
HT-14-2J-S-3	4.17	5.3×10^{17}	9,000	p
HT-14-2J-S-2	4.17	4.7×10^{17}	10,500	p

HT=Films deposited for heterojunction
ST=Source material thin film
Letter A,B,C,D indicate the source used. S is employed to designate the p-type stochiometric source.

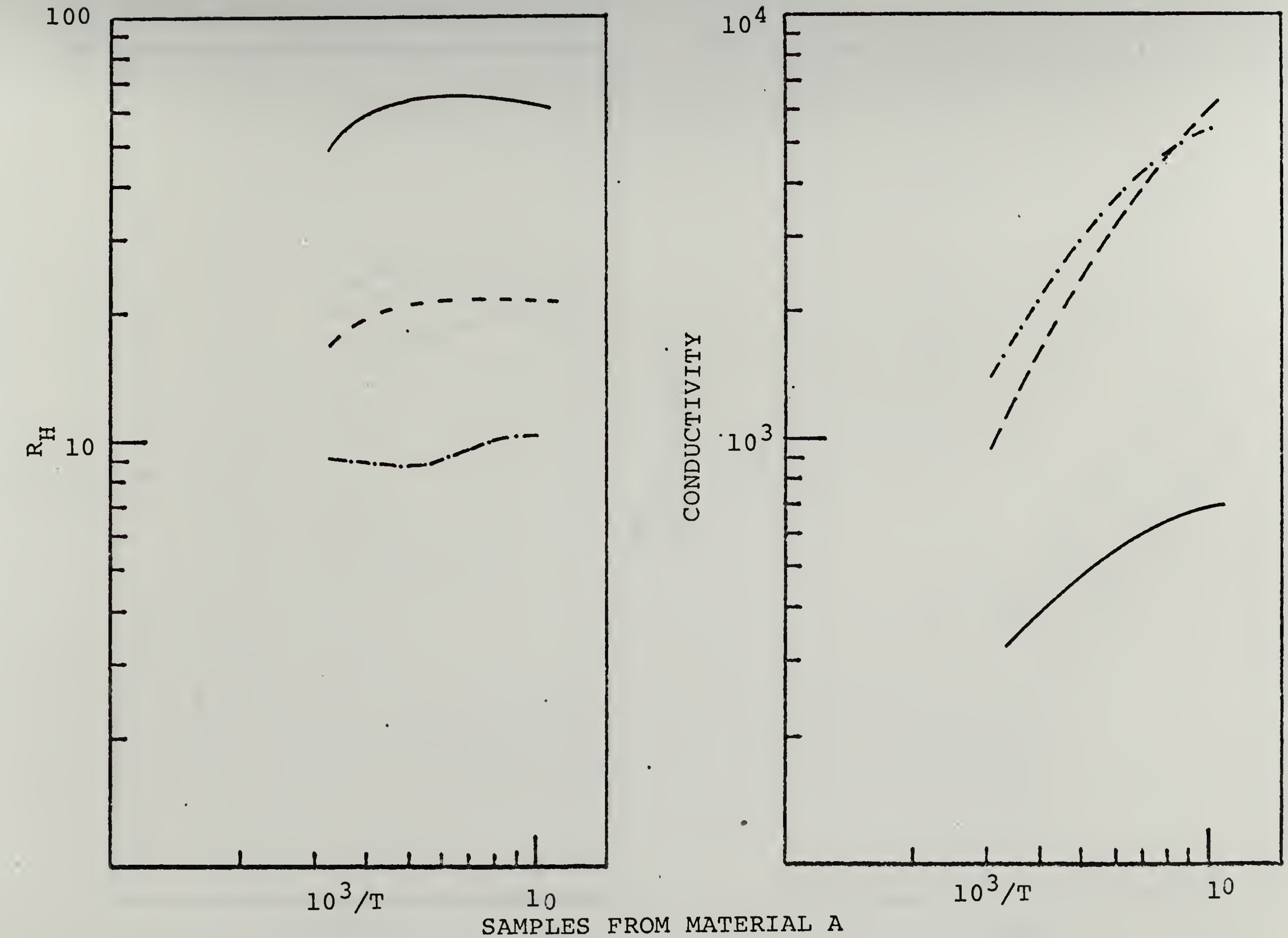

Figure 4.3 Hall Coeff and Conductivity versus Temperature for Material A

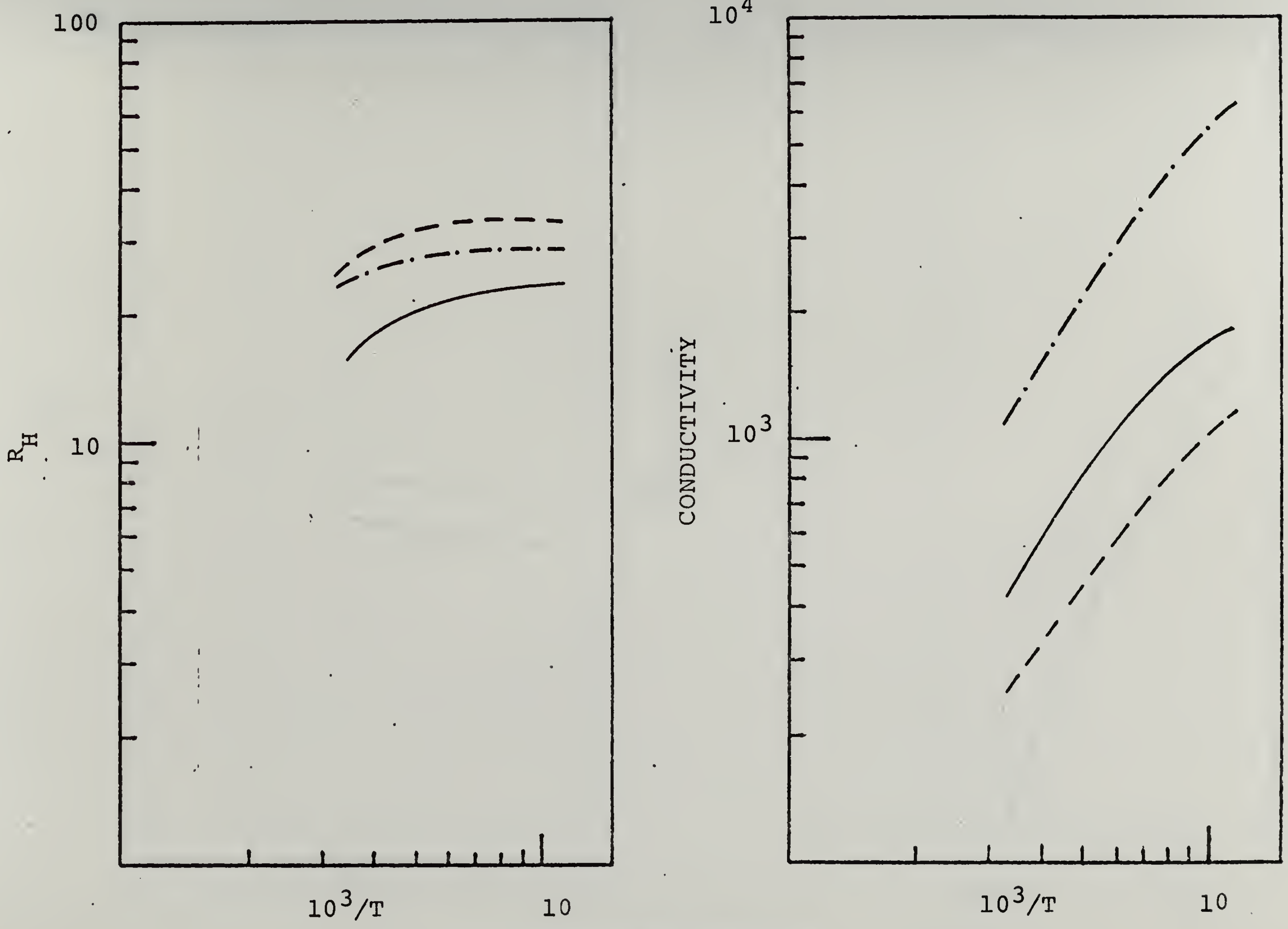

SAMPLES FROM MATERIAL B

Figure 4.4

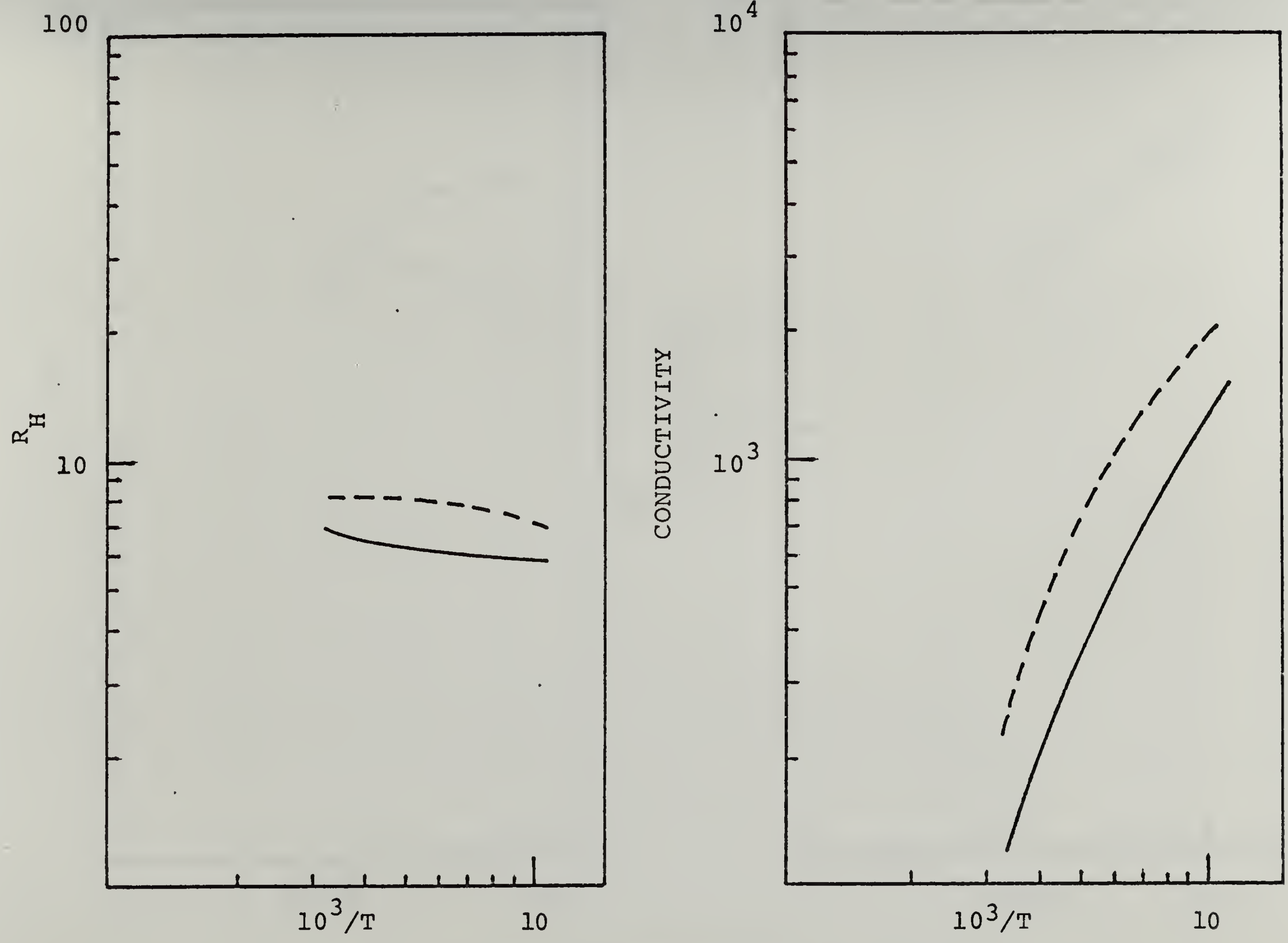

SAMPLES FROM MATERIAL C

Figure 4.5

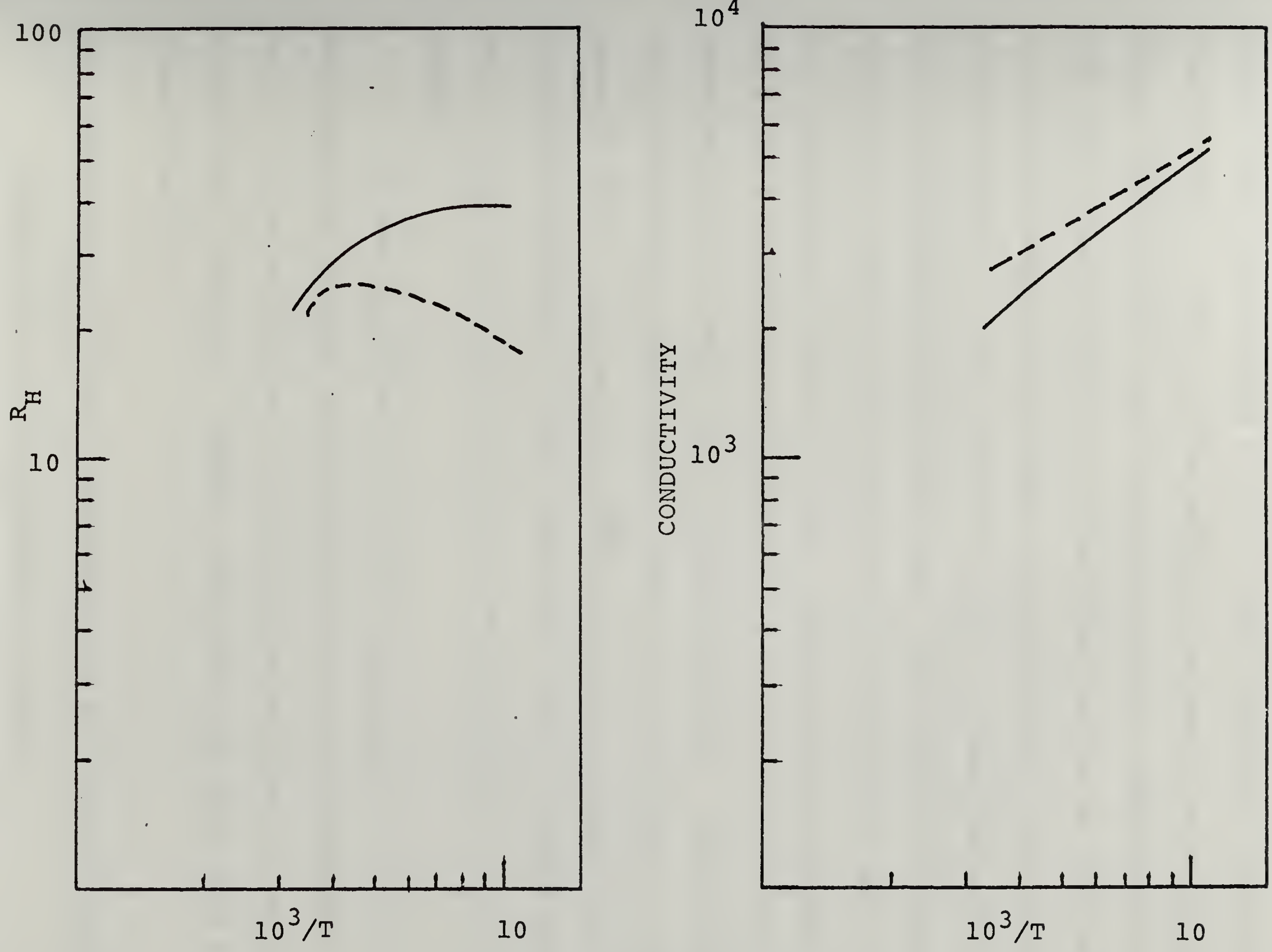

SAMPLES FROM MATERIAL D

Figure 4.6

Electrical measurements revealed that films using A,B, and D metal rich source materials are n type, but films using C source were unexpectedly p type. Such exception could have been caused by error in the weighing process, contamination during handling and quartz sealing process, inhomogenity in the alloy ingot or even an inconsistent nature of this metal rich source deposition process. Nevertheless, for a given source material, films obtained during the same deposition were consistently of the same type. The electrical properties measured at 90°K of films prepared from these four sources are presented in Table IV-I also. Using source materials A, B, C, D carrier combinations, in the low 10^{17}cm^{-3} have been obtained in some films without annealing. Mobilities vary considerably from 1000 to 11000 cm V Sac which is not unusual for Pb Sn Te thin films deposited on unpolished, unetched substrates. Films made from δ =0.04 source materials were n type with very high carrier concentrations in the 1 ^{19}cm^{-3} range.

It was suspected that source materials A, B, C, D had excessive oxides, another batches of source materials E, F, G, H were prepared with special care given to chemical etching and cleaning. However, they have not been used for deposition yet.

D. FABRICATION OF SINGLE HETEROJUNCTION $Pb_{1-x}Sn_xTe$ DIODES

1. Preparation of Heterojunction Layers

Two groups of single heterojunction $Pb_{1-x}Sn_x$ Te were prepared in this thesis study. Both were made of a p type

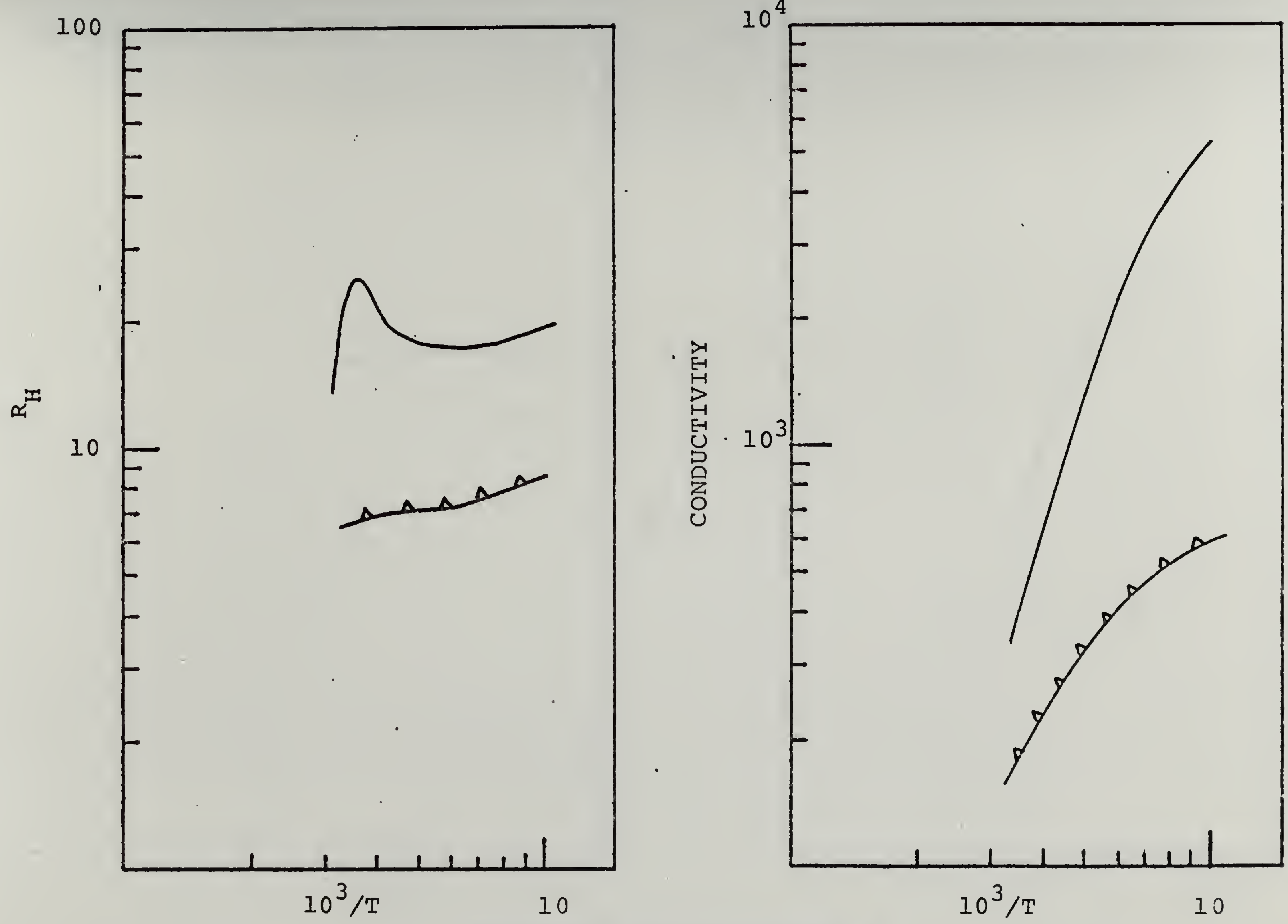

COMPONENTS HETEROJUNCTION 1

Figure 4.7

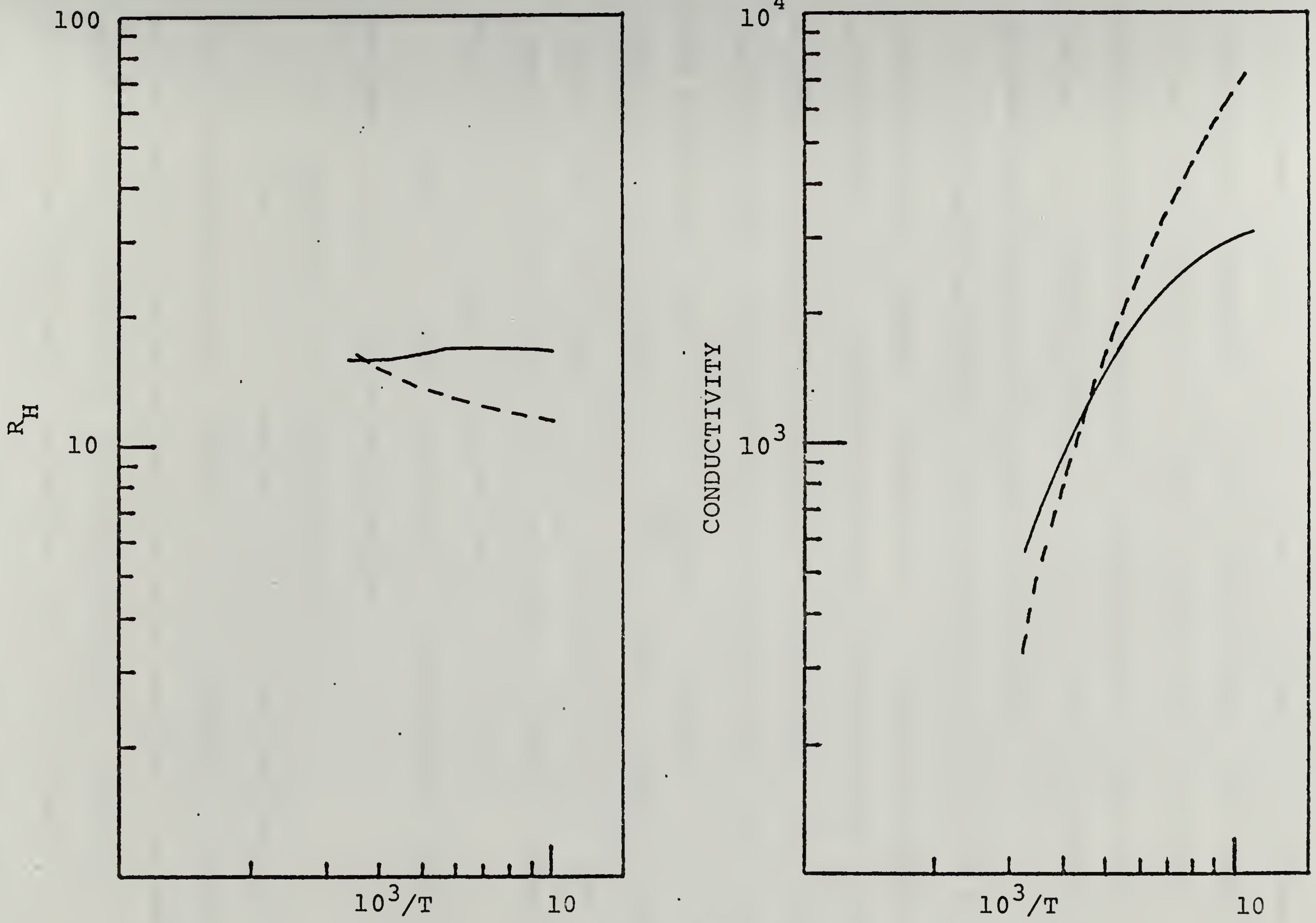

COMPONENTS HETEROJUNCTION 2

Figure 4.8

$Pb_{0.86}Sn_{0.14}Te$ layer and a n type $Pb_{0.80}Sn_{0.20}Te$ layer. In the first group, 5 μm thick p-layer was first deposited on KCl, followed by the second n layer of 10 μm in thickness using A source material. In the second group, the order of n layers was reversed. A 3.8 μm n layer using B source material was first deposited following by a 4.2 μm thick p-layer. In both depositions, p-layers were deposited using the same stoichiometric $Pb_{0.86}Sn_{0.14}Te$ source.

In each deposition, 2 KCl substrates were used to provide monitor samples. Consequently, after one deposition, two substrates were changed together with the source material. In order to minimize the oxidation of first layer when this change was made, the preparation of second deposition was done only after the deposition system was completely cooled down after first deposition, and the change of source material and substrates were made in only six minutes or so. The electrical properties of both the p and n layers of these tw heterojunction groups are presented in Table IV-I.

Finally, a gold deposition in the order of 5000 Å was made on top of the heterojunction.

2. Heterojunction Diode Fabrication

After trials of several different procedures, the one finally adopted was the use of a TO-5 header as holder of the sample. The heterojunction layer was cut into small square pieces by cleaving the KCl substrate. The small chips were mounted onto the header using silver epoxy. After drying, the KCl was dissolved with deionized water.

The wet TO-5 header with the diode was dried with helium gas. The exposed top side of the diode was connected to one of the electrical post of the TO-5 header by fine copper wire using silver epoxy.

Care must be given in the connection between the sample and the header to avoid overflow of silver epoxy at the edge of sample to short circuit the heterojunction. The sample area typically varied from 1 to 5 mm^2. A typical sample is shown in Figure 4.10.

E. I-V MEASUREMENT

The I-V rectification was evaluated on a Tektronix Model 541 Curve tracer with the sample dipped in liquid nitrogen. Most samples showed rectification. However, their hardness of rectification varied considerably. Some of the better characteristics taken directly from the curve tracer are shown in Figure 4.9 for two diodes, one of the first group and in one figure of the second group.

On selected samples, more detailed measurements of I-V characteristics were made as shown in Figure 4.12, from which the factor A which indicated the deviation from the ideal rectification and defined by $J=J_o e^{\frac{qV}{AkT}}$ can be determined from the straight forward bias of the log I versus linear V plot. A was found to vary from 5 to 10 in the diodes measured.

It should be strongly emphasized that there is a possibility that the rectification could come from the contact between silver epoxy and the top layer instead of or in

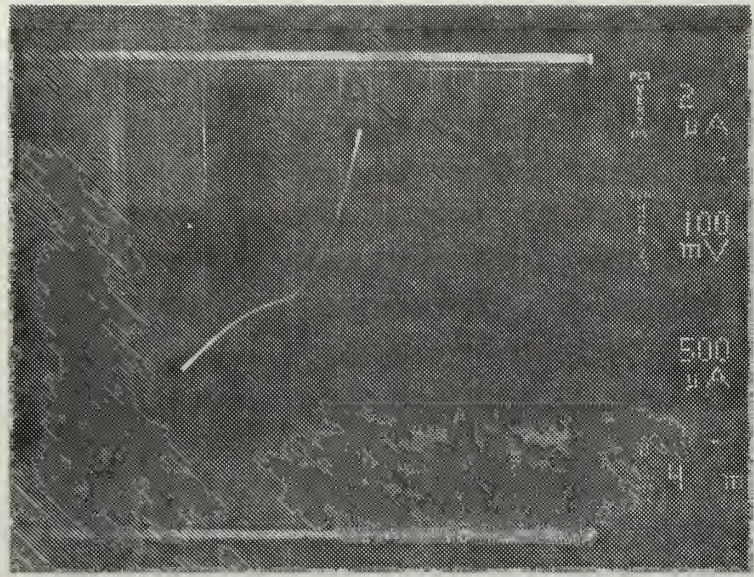

Diode 50

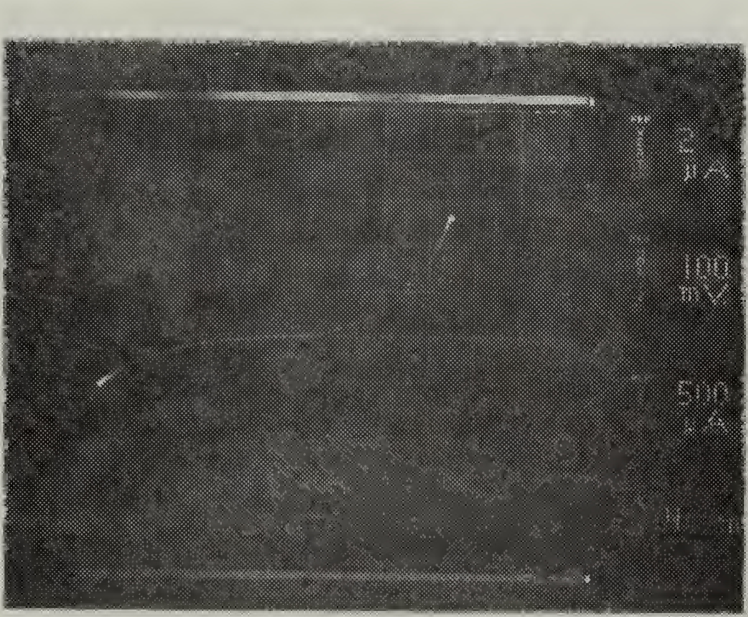

Diode 51

Figure 4.9 Rectification Curves for Diodes

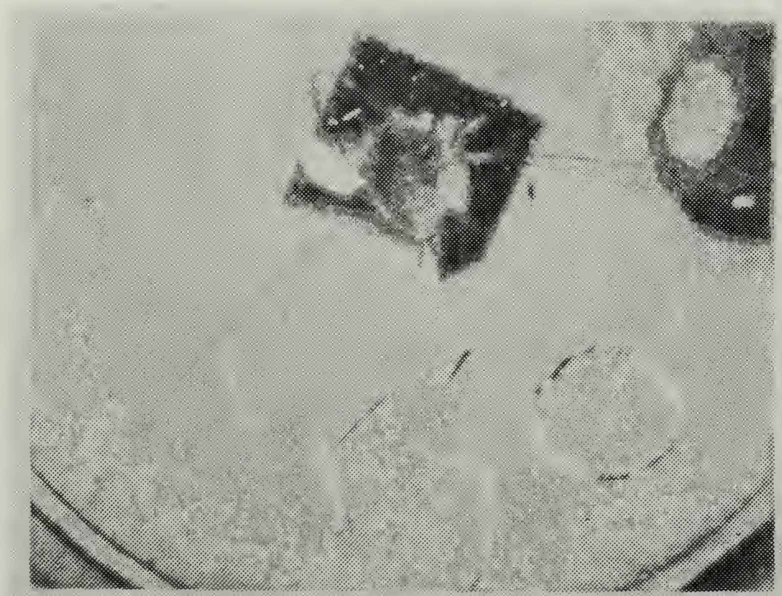

Diode Showing

Connector and Partial
part of the TO-5 header

Figure 4.10 Example of the Diode Fabricated

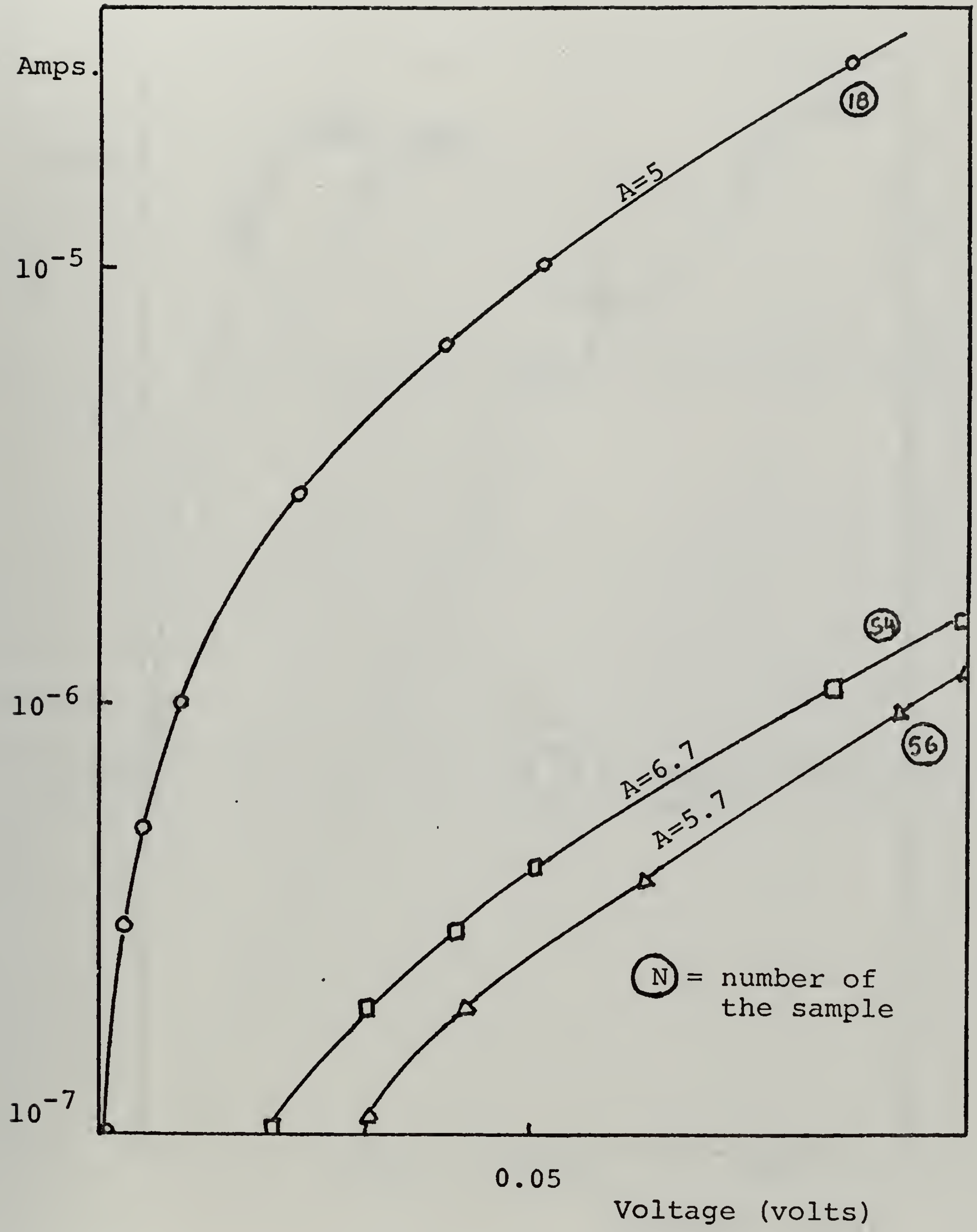

Figure 4.11 I-V Characteristic

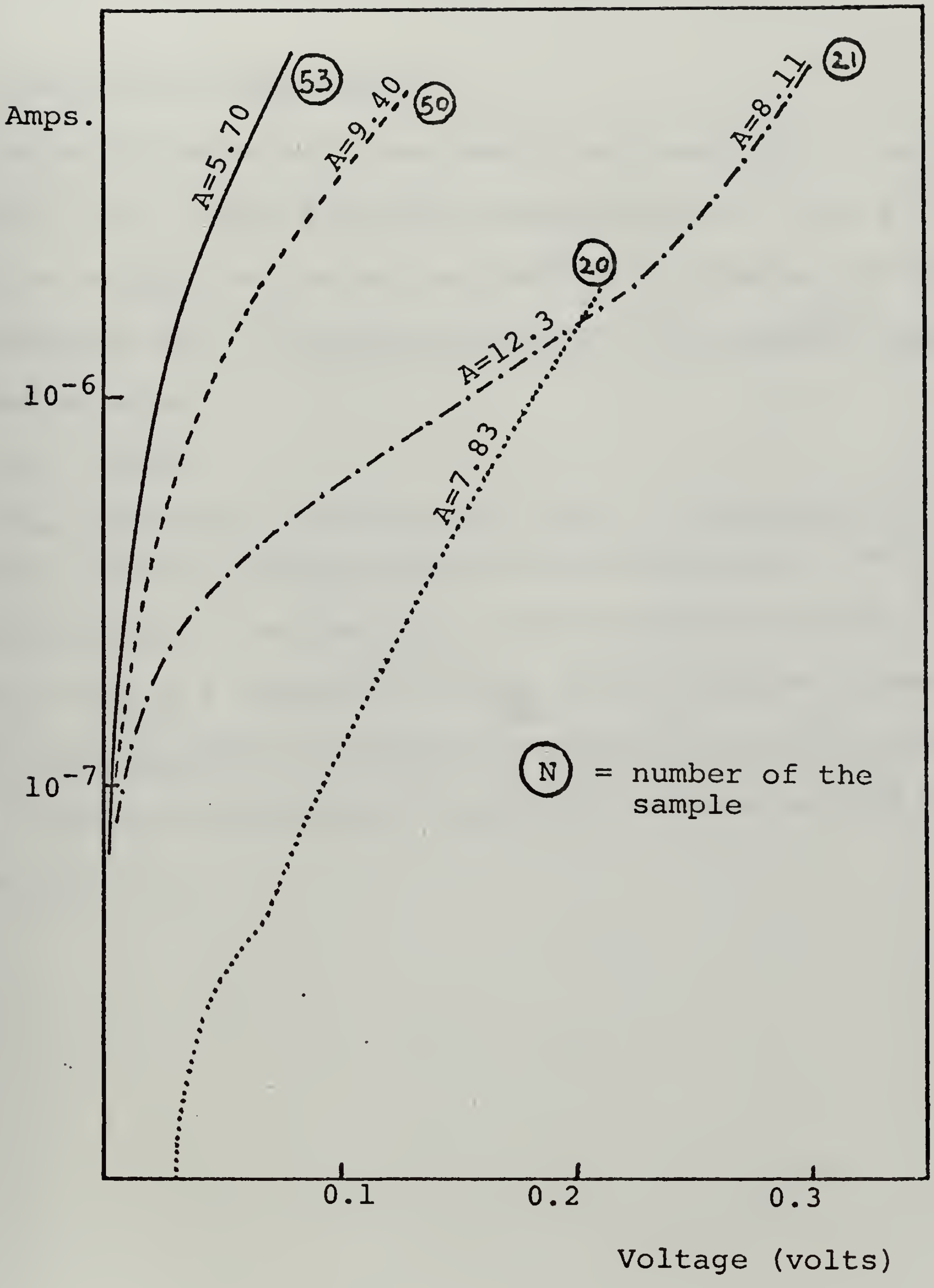

Figure 4.12 I-V Characteristics

addition to the rectification at the p-n heterojunction. Further investigations using silver epoxy on single p (or) layer are planned to examine such possibility.

F. CAPACITANCE MEASUREMENT

Capacitance of only one sample was measured at zero bias. It was 11 pf. More extensive measurements of C as a function of bias voltage are being carried out to examine the nature of junction and to determine whether it is abrupt, linearly graded or else.

G. R_oA VALUES

The qualityof a rectifying diode can be described by a figure of merit R_oA where R_o is the differential zero bias resistance and A is the diode cross sectional area. In Table IV-3, R_oA values of several SH $Pb_{1-x}Sn_xTe$ diodes at 77°K are presented. It should be pointed out that typical R_oA values of homojunction $Pb_{1-x}Sn_xTe$ diodes at 77°K have been less than 1-2.

TABLE IV-3

R_oA for Several Samples

SAMPLE	Ro (KΩ)	Area (mm^2)	R_oA (Ω-cm^2)
11	8.3	1.82	151.06
13	10.7	3.20	342.40
52	12.5	2.04	255.00
54	28.5	2.20	627.00
55	22.2	0.60	133.20
56	32.0	1.40	448.00
57	13.2	1.56	205.92
58	4.5	1.94	87.30

V. DESIGN OF A MULTI-SOURCE EVAPORATION SYSTEM

A. INTRODUCTION

In this thesis, single heterojunction $Pb_{1-x}Sn_xTe$ diodes were fabricated by a process which expose the first layer to atmosphere before the deposition of second layer. Although most of these diodes showed some degree of rectification. Some have very hard rectification and large R_oA products. It should be pointed out, however, that their photovoltaic properties and luminescent properties have not been tested. It is felt that the exposure to atmosphere most likely deteriorated the quality of interface. It seems to be an obvious improvement if several layers of different materials can be deposited sequentially without opening the vacuum system so that the surface of the layer will not be contaminated. A multi-source evaporation unit was designed. Most of the parts were fabricated. However, the mechanism of moving the substrate holder has not been completed which prevents the test of this new system before the writing of this thesis.

B. MULTI-SOURCE DESIGN

In this system, it was decided to make provisions for depositions of four materials. It may include three alloy semiconductor sources and one metal source for heterojunction fabrication. Or it may consist of two alloy semiconductor source, one e-gun source for insulator and one metal source for metal-insulator-semiconductor research.

A mock up of this system is shown in Figure 5.1. For each source section, cylindrical shield was provided to separate it from neighboring source sections and prevent the vapor from flowing all over the system.

For deposition of semiconductors, one boat method will be used. However, new feature of enclosing the vapor path between the source boat and substrate by a heated quartz tube was added. By heating the quartz chimney up to a temperature almost equal or even higher than the substrate temperature, it was felt that the deposition will be carried out in a quasi-equilibrium condition and improve the quality of thin films. This idea was developed by F. Bis and J. Dixon of the Naval Laboratory, White Oak, Maryland. (Ref. 30).

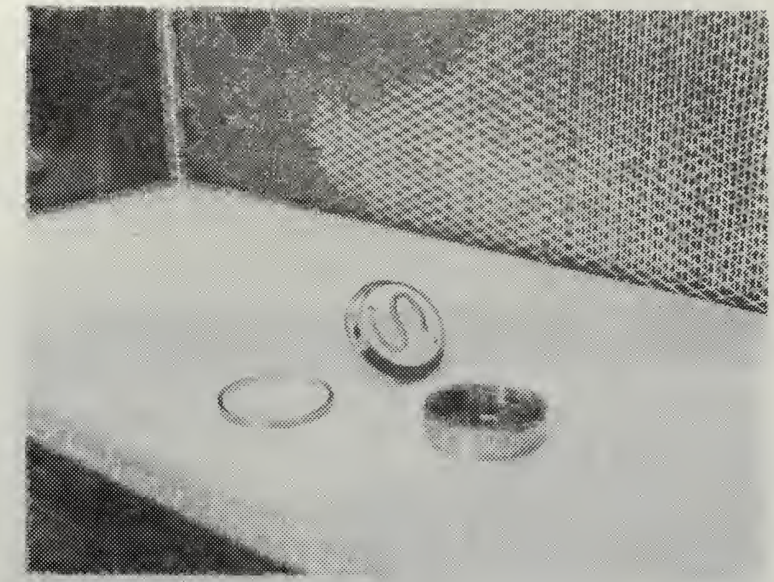

Substrate Holder

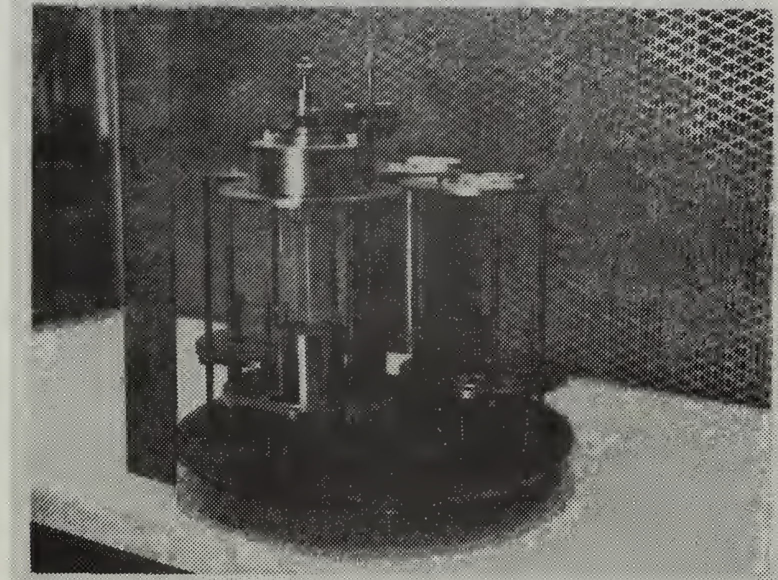

4 Multi-Source System

Figure 5.1 Multi-Source System

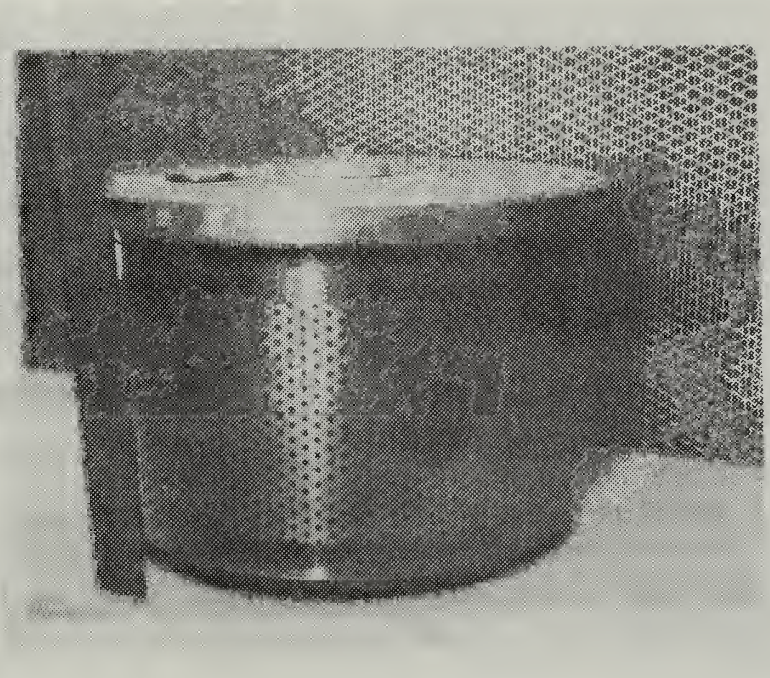

Flat Top Jar

Figure 5.1 Multi-Source System

VI. CONCLUSIONS AND RECOMMENDATIONS

A. CONCLUSION

Progress made during this thesis can be highlighted as follows:

1. N-type Films

Using metal rich source materials, it was found that n-type films can be developed with carrier concentration in the low 10^{17} cm^{-3} range without annealing. One of the metal rich source materials yielded p-type films indicating that better control of the preparation of ingot is needed.

2. Single Heterojunction $Pb_{1-x}Sn_xTe$ Diodes

It is most encouraging that over half of the SH diodes showed noticeable rectification although the hardness of their rectification curves varied considerably. It is believed that the procedure of making contact using silver epoxy gave inconsistent results. Most of the soft rectification could have been the consequence of high resistance contacts. However, it should be pointed out that SH diodes which have harder rectification than homojunction $Pb_{1-x}Sn_xTe$ diodes have been obtained. If R_oA product is used as a figure of merit, the good SH diodes have R_oA as high as 1000 which is at least two orders of magnitude higher than R_oA values of homojunction $Pb_{1-x}Sn_xTe$ diodes. This exciting result calls for urgent research to examine the photovoltaic, luminescence properties of these SH $Pb_{1-x}Sn_xTe$ diodes.

3. A simplified theoretical analysis has been carried out to calculate the laser performance of double heterojunction $Pb_{1-x}Sn_xTe$ diodes. Its results will be used as guides for the experimental development of DH $Pb_{1-x}Sn_xTe$ devices.

B. RECOMMENDATIONS

The following improvements can be made:

1. It is most interesting to examine the possible improvements using the multi-source deposition system in fabricating heterojunctions without exposing the sample surface to atmosphere between layers.

2. Preparation of source materials should be improved by properly etching away the oxides and even considering zone refining the alloy.

3. It is important to examine at the earliest possibility whether there is rectification between the silver epoxy and the contact with the $Pb_{1-x}Sn_xTe$ layer instead of, or in addition to, rectification at the hetrojunction interface.

4. Silver epoxy contact does not seem to be satisfactory although good rectification characteristics have been obtained. Other contacting methods such as indium deposition, gold thalium alloys, platinum deposition, etc., should be tried.

5. As for the theoretical analysis, it will be very helpful to apply the theoretical calculation to homojunction $Pb_{1-x}Sn_xTe$ laser diodes using the parameters selected for this SH diode calculation and examine if these values are correct estimates.

(This page intentionally blank)

LIST OF REFERENCES

1. Dimmock, J. O., Melngailis, J., and Strauss, J., "Band Structure and Laser Action in $Pb_{1-x}Sn_xTe$." Phys. Rev. Ltrs., 16:1193-1196, June 27, 1966.

2. Strauss, A. J., "Inversion of Conduction and Valence Bands in $Pb_{1-x}Sn_xSe$ Alloys." Phys. Rev., 157:608-611, May 1967.

3. Melngaillis, I., "Laser Action and Photodetection in Lead-Tin Chalcogenides." Journal de Physique, (Proceedings of International Colloquim on IV-VI Compounds), 29:64-84, 1968.

4. Strauss, A. J., "Metallurgical and Electronic Properties of $Pb_{1-x}Sn_xTe$, $Pb_{1-x}Sn_xSe$, and Other IV-VI Alloys." Trans. Metall. Soc. AIME., 242:354-365, March 1968.

5. Tao, T. F., Wang, C. C., and Kasai, I., "Optical Energy Gap of $(PbSe)_{1-z}(SnTe)_z$ Alloys." Paper presented at the Conference on the Physics of Semimetals and Narrow Gap Semiconductors. The American Physical Society, March 20-21, 1970, Dallas, Texas.

6. Butler, J. F., and Clawa, A. R., Physics of Quantum Electronics. p. 438-466, McGraw-Hill, 1966.

7. Nikolic, P. M., "Optical Energy Gaps, Lattice Parameters and Solubility Limits of Solid Solutions of SnSe and GeSe in PbTe, and GeSe in SnTe." Brit. J. Appl. Phys., 16:1075-1079, August 1965.

8. Bylander, E. G., "Reproducible Preparation of $Pb_{1-x}Sn_xTe$ Epitaxial Films with Moderate Carrier Concentrations" Mater. Sci. and Engr., 1:190-194, September 1966.

9. Walz, V. M., The Determination of Optical Properties and Energy Gap of $Pb_{1-x}Sn_xTe$ Thin Films in the Fundamental Absorption Edge Region. M. Thesis, Naval Postgraduate School, Monterey, California, 1972.

10. Melngailis, I., and Calawa, A. R., "Photovoltaic Effect in $Pb_{1-x}Sn_xTe$ Diodes." Appl. Phys. Ltrs., 9:304-306, October 15, 1966.

11. Melngailis, I., and Harman, T. C., "Photoconductivity in Single Crystal $Pb_{1-x}Sn_xTe$." Appl. Rev. Ltrs., 13:180-183, September 1, 1966.

12. Esaki, L., and Stiles, P. J., "New Type of Negative Resistance in Barrier Tunneling." Phys. Rev. Ltrs, 16:1108-1111, June 13, 1966.

13. Hoff, G. F., Band Inversion and the Electrical Properties of Lead-Tin-Selenide Semiconducting Alloys. Ph.D. Thesis, University of Maryland, College Park, Maryland, 1970.

14. Calawa, A. R., Harman, T. C., Finn, M., and Youtz, P., "Crystal Grotw, Annealing and Diffusion of Lead-Tin Chalcogenides." Trans. Metall. Soc. AIME., 242:374-383, March 1968.

15. Technical Staff, "Electronics International." Electronics, p. 66-67, March 2, 1970.

16. Wagner, J. W., and Willardson, R. K., "Growth and Characterization of Single Crystals of PbTe-SnTe." Trans. Metall. Soc. AIME., 242:366-371, March 1968.

17. Thompsom, A. G., and Wagner, J. W., "The Growth of $Pb_{1-x}Sn_xTe$ by Liquid Epitaxy." Paper presented at the 16th National Symposium. The American Vacuum Society. October 28-31, 1969, Seattle, Washington.

18. Anderson, R. L., "Experiments on GeGaAs Heterojunctions." Solid State Electron. 5:p. 341, 1962.

19. Sze, S. M., Physics of Semiconductor Devices., p. 102-104, Wiley, 1969.

20. Rediker, R. H., Stopek, S., and Ward, J. H. R., Interfac-Alloy Epitaxial Heterojunctions." Solid State Electron., 7, p. 621, 1964.

21. Hinkley, E. D., and Rediker, R. H., "GaAs-InSb Graded-Gap Heterojunction." Solid State Electron., 10, p. 671, 1967.

22. Shewchun, J., and Wei, L. Y., "Germanium-Silicon Alloy Heterojunction." J. Electrochemical Soc., 111, p. 1145, 1964.

23. Adams, M. J., and Landsberg, P. T., Gallium Arsenide Lasers, p. 61, Wiley, 1969.

24. Sleger, K. J., McLane, G. F., and Mitchell, D. L., Calculation of the Optical Confinement in $PbS_{1-x}Se_x$ Double Heterojunction Laser., from the Naval Research Laboratory, Washington, D. C., paper not published yet.

25. Anderson, W. W., "Mode Confinement and Gain in Junction Lasers." J. Quantum Electron., vol. QE-1, No. 6, p. 228-236, September 1965.

26. Adams, M. J., and Cross, M., "Electromagnetic Theory of Heterostructure Inyection Lasers." Solid State Electron., 14, p. 865-883, 1971.

27. Kressel, H. Lasers, Chapter 1, Marcel Dekker, Inc., 1971.

28. Logothetis, E. M., Holloway, H., Varga, A. J., and Wilkes, E., "Infrared Detection by Schottky Barriers in Epitaxial PbTe." Appl. Phys. Letters., vol. 19, No. 9, p. 318-320, November 1, 1971.

29. Air Force Materials Laboratory, Report AFML-TR-71-238, and School of Engineering and Applied Science, University of California, Los Angeles, California. Narrow Gap Semiconductors - $Pb_{1-x}Sn_xTe$ and $Pb_{1-y}Sn_ySe$.", by T. F. Tao and C. C. Wang.

INITIAL DISTRIBUTION LIST

		No. Copies
1.	Defense Documentation Center Cameron Station Alexandria, Virginia 22314	2
2.	Library, Code 0212 Naval Postgraduate School Monterey, California 93940	2
3.	Asso. Professor T. F. Tao Department of Electrical Engineering Naval Postgraduate School Monterey, California 93940	5
4.	Teniente 1° Jose M. Fernandez E. OFROL 953 Direccion General del Personal de la Armada Prat 620. Valparaiso Chile	1

DOCUMENT CONTROL DATA - R & D

(Security classification of title, body of abstract and indexing annotation must be entered when the overall report is classified)

1. ORIGINATING ACTIVITY *(Corporate author)* Naval Postgraduate School Monterey, California 93940	2a. REPORT SECURITY CLASSIFICATION Unclassified 2b. GROUP

3. REPORT TITLE

Study of Heterojunction $Pb_{1-x}Sn_xTe$ Diodes

4. DESCRIPTIVE NOTES *(Type of report and, inclusive dates)*
Master's Thesis; December 1972

5. AUTHOR(S) *(First name, middle initial, last name)*

Jose Manuel Fernandez

6. REPORT DATE	7a. TOTAL NO. OF PAGES	7b. NO. OF REFS
December 1972	84	29

8a. CONTRACT OR GRANT NO.	9a. ORIGINATOR'S REPORT NUMBER(S)
b. PROJECT NO.	
c.	9b. OTHER REPORT NO(S) *(Any other numbers that may be assigned this report)*
d.	

10. DISTRIBUTION STATEMENT

Approved for public release; distribution unlimited.

11. SUPPLEMENTARY NOTES	12. SPONSORING MILITARY ACTIVITY
	Naval Postgraduate School Monterey, California 93940

13. ABSTRACT

A new procedure of using metal rich $(Pb_{1-x}Sn_x)_{1+}$ Te alloy source in a graphite boat deposition method has been developed in preparing n-type $Pb_{0.8}Sn_{0.2}Te$ thin films of carrier concentration in the low 10^{17} cm^{-3} range without annealing. Using this procedure, single heterojunction $Pb_{1-x}Sn_xTe$ diodes have been made by sequential depositions of p-type $Pb_{0.86}Sn_{0.14}Te$ and n-type $Pb_{0.80}Sn_{0.20}Te$ thin films on cleaved (100) KCL substrates. Diodes were made by using gold deposition and silver epoxy contacts. Rectifying diodes of R_oA values as high as 600 ohm-cm^2 have been obtained.

A theoretical analysis was carried out in calculating the laser performance of a double heterojunction $Pb_{1-x}Sn_xTe$ diodes. Its results will be used as guidelines for continuing experimental research and development.

DD FORM 1 NOV 65 1473 (PAGE 1)
S/N 0101-807-6811

A-31408

UNCLASSIFIED

Security Classification

14. KEY WORDS	LINK A		LINK B		LINK C	
	ROLE	WT	ROLE	WT	ROLE	WT
Heterojunction $Pb_{1-x}Sn_xTe$						

D FORM 1 NOV 65 1473 (BACK)

/N 0101-807-6821

UNCLASSIFIED

Security Classification

A-31409

Thesis 143141
F262 Fernandez
c.1 Study of heterojunction $Pb_{1-x}Sn_xTe$ diodes.